Utrecht University

Bachelor's Thesis
Mathematics and Physics

Braid Groups

Author:
Dennis Hilhorst

Supervisors:
Dr. Lennart Meier
Dr. Dirk Schuricht

June 15, 2021

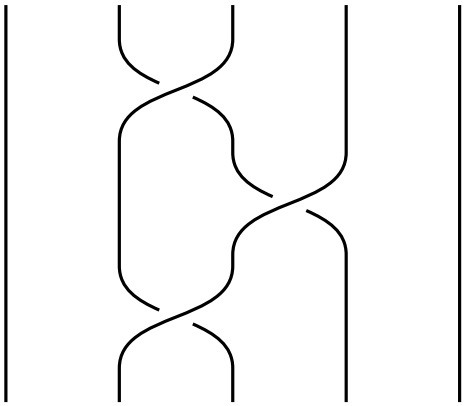

Utrecht University

Abstract

In this thesis we will be looking at braid groups, their representations and how they play a role in quantum mechanics in two dimensions. We introduce configuration spaces, and prove a theorem by Artin relating the Artin braid groups B_n to braids on $\mathbb{R}^2$. We consider the Burau representation and the Lawrence-Krammer-Bigelow representation and give an idea of their derivations. We discuss the relevance of braid groups for anyons in two dimensional space, and discuss their realization in the Fractional Quantum Hall Effect. Finally, we see how we might obtain braid group representations from category theory.

Contents

Chapter 0

Introduction

Braid groups were first explicitly introduced by Emil Artin in the 1920s, to study the intertwining of strings in three-dimensional space. He showed that braids with a fixed number of strands, n, formed a group B_n [1]. The braid groups have interesting algebraic and topological properties, which we will look at in this thesis. Braid structures also appear in other areas in mathematics and physics. One important occurrence of braiding in physics is the existence of anyons, a term coined by Frank Wilczek [2]. Anyons are particles with statistics different from bosons or fermions. Another example is that of braided monoidal categories, introduced by Joyal and Street [3], which can even be used to derive braid group representations.

In the first chapter of this thesis, we will provide a basic introduction to braid groups. We point out some basic properties, and introduce braid diagrams. In the second chapter, we will introduce configuration spaces, and an important theorem due to Artin. This theorem shows that the Artin braid groups are in fact homotopy groups of the configuration spaces of indistinguishable particles moving around on the plane. We will also consider braid groups on other manifolds, and basic examples of those. In the third chapter, we will look at some representations of the braid groups, arising from topology, mainly the Burau representation and the Lawrence-Krammer-Bigelow representation. In the fourth chapter, we will study anyons, and see how they relate to braid groups on manifolds. We will also introduce the abstract construction by Leinaas and Myrheim [4], and a physical construction by Frank Wilczek [2]. After this, we look at the Fractional Quantum Hall Effect (FQHE), and how anyons play a role there. In the fifth and final chapter, we take a short look at braid structures in category theory, and how they might be used to construct braid group representations.

One thing I found particularly interesting to note was how easily braid structures might be overlooked when certain symmetries are assumed. Joyal and Street mention this in their article when motivating braided monoidal categories, writing that "it has been consistently felt that the symmetry condition $c_{BA}c_{AB} = 1_{A\otimes B}$ should be assumed" regarding commutativity of tensor products [3]. Leinaas and Myrheim mention something in a similar vein when introducing their article, stating that that "indistinguishability of particles is expressed in the theory by imposing symmetry constraints on the state functions and observables" [4]. They point out that such constraints are in agreement with experiments, but not very well justified in the theory.

Chapter 1

Braid Groups

To start things off, we will introduce the main objects of interest of this thesis: braid groups. In this chapter we will introduce the braid groups and some basic properties and related definitions.

The braid group on n strands is the group B_n, also known as the Artin braid group, defined for any positive integer n. Their algebraic definition is as follows [1].

Definition 1.1. *The Artin braid group B_n is the group generated by $n-1$ generators $\sigma_1, \sigma_2, \ldots, \sigma_{n-1}$ with the following relations:*

$$\sigma_i \sigma_j = \sigma_j \sigma_i \tag{B1}$$

for all $i, j = 1, 2, \ldots, n-1$ with $|i-j| \geq 2$, and

$$\sigma_i \sigma_{i+1} \sigma_i = \sigma_{i+1} \sigma_i \sigma_{i+1} \tag{B2}$$

for all $i = 1, 2, \ldots, n-2$.

One can note that B_1 has no generators, and is thus a trivial group, and that B_2 has one generator of infinite order, so $B_2 \cong \mathbb{Z}$.

Another common, more visually appealing way to define braids is by using *braid diagrams*. An example can be seen in Figure 1.1. Braid diagrams can be seen as a subset of $\mathbb{R}^2 \times I$ with $I = [0, 1]$, a union of n intervals, called the strands. We draw the projection on $\mathbb{R} \times I$ to see which strand goes over which. The strand that goes under another at a crossing is discontinued at that crossing. The endpoints of the strands are the points

$$\{\, (1,0,0), (2,0,0), \ldots, (n,0,0) \,\} \quad \text{and} \quad \{\, (1,0,1), (2,0,1), \ldots, (n,0,1) \,\}$$

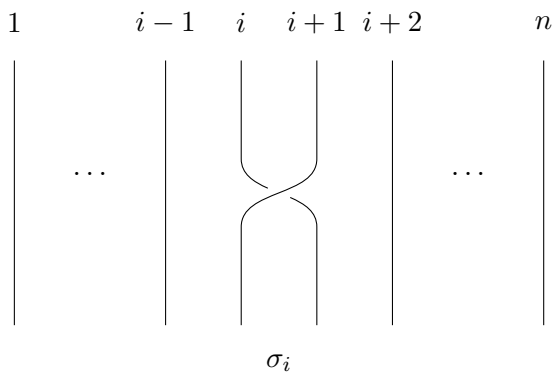

Figure 1.1: An example of a braid diagram with the generator σ_i.

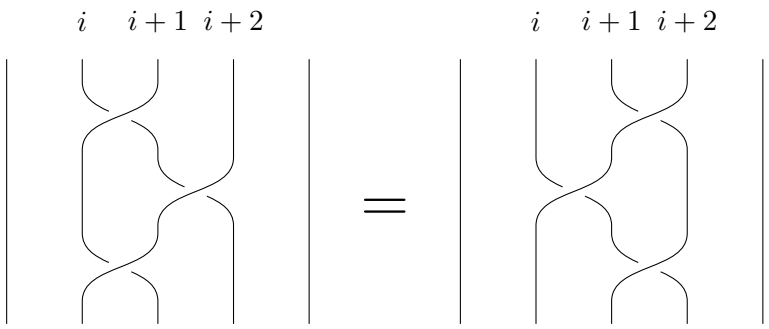

Figure 1.2: The braid relation (B2). This equivalence is also known as the Reidemeister move Ω_3.

In braid diagrams, for convenience sake, we require that at most two strands cross at any point. This is not a necessary requirement, but it is equivalent and much more convenient. If we see braid diagrams as subsets of $\mathbb{R} \times I$ we then require the following things:

(i) The projection $\mathbb{R} \times I \to I$ maps each strand homeomorphically onto I. This simply means all strands are disjoint.

(ii) Every point of $\{ 1, 2, \ldots, n \} \times \{ 0 \} \times \{ 0, 1 \}$ is the endpoint of a unique strand. We cannot have multiple strands connecting to one endpoint.

(iii) Every point of $\mathbb{R} \times I$ belongs to at most two strands. One of them is distinguished and is said to be *undergoing*, the other strand is *overgoing*. This is the requirement that only two strands cross at any point.

(iv) Every strand crosses every plane $\mathbb{R}^2 \times \{ x \}$ with $x \in I$ precisely once. This essentially means that strands only go in one direction. We do not draw strands that go up and then back down again, only to go back up after that. This requirement is not necessary, but it is convenient and equivalent [5, Page 7].

It can easily be verified that relation (B1) must hold, and for the second braid relation, one can draw a diagram to make it more clear (see Figure 1.2). Intuitively, one can see that the right hand side can be obtained from the left hand side by shifting the strand starting on i down, the strand starting on $i + 1$ to the right and the strand starting on $i + 2$ up.

1.1 Some basic properties

Braid groups are strongly related to the symmetry groups S_n. In fact, the braid group B_n can be projected onto the symmetry group S_n. More generally, we can prove the following [1].

Lemma 1.2. *If $s_1, \ldots, s_{n-1}$ are elements of a group G, satisfying the braid relations, then there is a unique group homomorphism $f : B_n \to G$ such that $s_i = f(\sigma_i)$ for all $i = 1, 2, \ldots, n - 1$.*

Proof. Let $\mathcal{F}_n$ be the free group on the generators $\{ \sigma_1, \sigma_2, \ldots, \sigma_n \}$. Then consider the unique homomorphism $\overline{f}$ defined by

$$\overline{f} : \mathcal{F}_n \to G : \overline{f}(\sigma_i) = s_i$$

for $i = 1, 2, \ldots n$. Now, B_n is defined by the braid relations on a set of generators. Let $N \trianglelefteq \mathcal{F}_n$ be the smallest normal subgroup containing the elements rr'^{-1} for all braid relations $r = r'$ (B1) and (B2). This is the union of all conjugacy classes of the relations rr'^{-1}. Then B_n is defined as $\mathcal{F}_n/N$.

Note that $\overline{f}(N) = \{ 1 \} \leq G$. After all, the image of any element rr^{-1} is identity, so the image of any conjugate of such an element is too. This can be verified by straightforward computation. Take $i, j = 1, 2, \ldots, n$ with $|i - j| \geq 2$. Then

$$\overline{f}(\sigma_i\sigma_j\sigma_i^{-1}\sigma_j^{-1}) = \overline{f}(\sigma_i)\overline{f}(\sigma_j)\overline{f}(\sigma_i^{-1})\overline{f}(\sigma_j^{-1}) = s_is_js_i^{-1}s_j^{-1} = s_js_is_i^{-1}s_j^{-1} = 1$$

since the first braid relation holds in G. A similar thing can be done for the braid relation (B2). This means we have

$$N \leq \ker \overline{f} \trianglelefteq \mathcal{F}_n$$

Then by the isomorphism theorems there is a surjective homomorphism

$$B_n \cong \mathcal{F}_n/N \to \mathcal{F}_n/\ker \overline{f} \cong \overline{f}\left(\mathcal{F}_n\right),$$

defined by sending $\sigma_i N$ to $\sigma_i \ker \overline{f}$. In this way, $\overline{f}$ induces a homomorphism from B_n to G, sending $\sigma_i N$ to s_i. □

We can apply this lemma to $G = S_n$, where $s_i = (i, i+1)$, the transposition exchanging i and $i+1$, to find a group homomorphism

$$\nu : B_n \to S_n \tag{1.1}$$

that projects B_n onto S_n. It can be easily verified that the s_i fulfill the braid relations, and thus the lemma applies. Since the s_i generate S_n, this homomorphism is surjective.

An intuitive idea for this fact is that we can obtain permutations in S_n by simply following the strands in the corresponding braid diagrams for B_n. For example follow the strands of the generator σ_i seen in Figure 1.1. The strands connect i to $i+1$, and $i+1$ to i, much like s_i would exchange i and $i+1$.

A direct consequence of this is the following lemma.

Lemma 1.3. *The group B_n with $n \geq 3$ is non-abelian.*

Proof. Let $n \geq 3$ be given. Suppose B_n is abelian, and consider the projection ν from (1.1). Then

$$\nu(\sigma_i\sigma_{i+1}) = s_is_{i+1},$$

but also

$$\nu(\sigma_i\sigma_{i+1}) = \nu(\sigma_{i+1}\sigma_i) = s_{i+1}s_i,$$

by our assumption. However, $s_is_{i+1} \neq s_{i+1}s_i$ in S_n. This is a contradiction, and B_n must be non-abelian. □

Another important property is that the braid groups can be naturally included in braid groups of more strands. In other words, the group homomorphism

$$\iota : B_n \to B_{n+1} : \sigma_i \mapsto \sigma_i \tag{1.2}$$

is injective. One can think of this as taking any braid diagram of B_n, and adding an extra $n+1$-th strand to it on the right. The proof of this given in [1] is given in the context of geometric braids, the study of braid diagrams as subsets of $\mathbb{R}^2 \times I$ with I an interval.

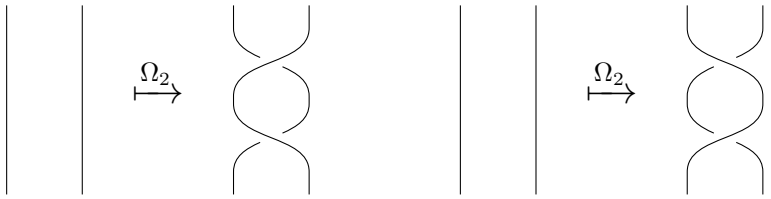

Figure 1.3: The Reidemeister move Ω_2.

1.2 Geometric braids

The idea behind geometric braids is that we don't view braids as purely algebraic, but as a subset b of $\mathbb{R}^2 \times I$, with $I = [0, 1]$ an interval.

Definition 1.4. *A geometric braid on $n \geq 1$ strands is a set $b \subset \mathbb{R}^2 \times I$ formed by n disjoint topological intervals (strands), such that the projection $\mathbb{R}^2 \times I \to I$ maps each strand homeomorphically onto I and*

$$b \cap (\mathbb{R}^2 \times \{\, 0 \,\}) = \{\, (1,0,0), (2,0,0), \ldots, (n,0,0) \,\}$$
$$b \cap (\mathbb{R}^2 \times \{\, 1 \,\}) = \{\, (1,0,1), (2,0,1), \ldots, (n,0,1) \,\}$$

So basically, the ends of a geometric braid connect the a permutation of the points they started. The other requirement is essentially saying that different strands cannot intersect. The product of 2 braids is defined as laying one behind the other. If we have two geometric braids $b_1, b_2 \subset \mathbb{R}^2 \times I$, then $b_1 b_2$ is the set of points $(x, y, t) \in \mathbb{R}^2 \times I$ where $(x, y, 2t) \in b_1$ if $t \leq \frac{1}{2}$ and $(x, y, 2t - 1) \in b_2$ if $t \geq \frac{1}{2}$.

We depict the braid diagrams as 2 dimensional pictures, while they should actually be 3 dimensional. The issue is in the crossings. In braid diagrams, we leave out a small part of the strand that goes behind another strand in the diagram. One can rigorously prove that braid diagrams represent equivalent braids if they are equivalent up to finite sequences of isotopy (continuous transformation of one braid diagram into another) and *Reidemeister moves* Ω_2 and Ω_3. Ω_3 is depicted in Figure 1.2, Ω_2 is depicted in Figure 1.3.

The idea for this proof is to first show that the braids are always at least a small distance ϵ away from each other. Then instead of the actual braids, we consider *polygonal braids*. Polygonal braids are connected line segments and nodes that correspond to the original braid. We can cut up the braid into enough segments that they all lie less than a distance ϵ away from the original braid. Proving things about these chains of line pieces is simpler. Instead of continuous isotopy, one only considers the "polygonal equivalent" of this: Δ-moves. With a Δ-move, a line segment is replaced by 2 line segments connecting a new node. For a complete proof, I refer to theorem 1.6 in [1].

An interesting result from this theorem is that it in fact does not matter whether for σ_i we choose if strand i goes over $i + 1$, or vice versa, the mathematics works out the same (in other words: one can exchange σ_i for σ_i^{-1} and obtain the same results).

1.3 Pure braids

An important subgroup of the braid group is the group of *pure braids*. The pure braid group on n braids P_n is defined as

$$P_n = \ker(\nu : B_n \to S_n). \tag{1.3}$$

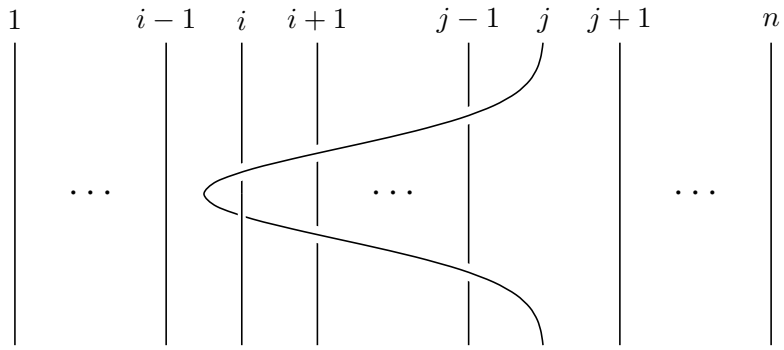

Figure 1.4: The pure n string braid $A_{i,j}$ with $1 \leq i < j \leq n$.

In other words: a pure braid is a braid that corresponds to the identity permutation, so a strand in a pure braid starting at $(i, 0, 0)$ ends at $(i, 0, 1)$. We can define certain important braids in the pure braid groups, called the *pure n-string braids* $A_{i,j}$, seen in Figure 1.4.

In terms of generators, they are defined as

$$A_{i,j} = \sigma_{j-1}\sigma_{j-2} \dots \sigma_{i+1}\sigma_i^2\sigma_{i+1}^{-1} \dots \sigma_{j-2}^{-1}\sigma_{j-1}^{-1}, \tag{1.4}$$

for $1 \leq i < j \leq n$. One can check that using

$$\alpha_{i,j} := \sigma_{j-1}\sigma_{j-2} \dots \sigma_i,$$

these $A_{i,j}$ are conjugate to one another in B_n as $A_{j,k} = \alpha_{j,k} A_{i,j} \alpha_{j_k}^{-1}$ (either by filling in the definitions or by drawing a picture). It turns out that the following holds.

Theorem 1.5. *P_n is generated by the $\frac{n(n-1)}{2}$ elements $\{ A_{i,j} \}_{1 \leq i < j \leq n}$.*

The proof for this theorem is quite long, we can give an idea for it.

Proof Idea. Much like the embedding $\iota : B_n \to B_{n+1}$, we can define a similar sort of map called a *forgetting homomorphism*

$$f_n : P_n \to P_{n-1},$$

which "forgets" the n-th strand, or in other words: removes it from the braid diagram. Observe

$$U_n := \ker(f_n).$$

It is obvious that $A_{i,n} \in U_n$. After all, removing the n-th strand from $A_{i,n}$ leaves a trivial braid. In fact, one can show that the U_n are free on the generators $\{ A_{i,n} \}$. From the definition of U_n, it follows that any braid β in P_n can be written as

$$\beta = \iota(\beta')\beta_n,$$

with $\beta_n \in U_n$ and $\beta' = f_n(\beta)$. Inductively, this means that

$$\beta = \beta_1\beta_2 \dots \beta_n,$$

and since the β_j are in U_j, which is generated by $A_{i,j}$ for $1 \leq i < j$, it follows that the theorem holds. I refer to [1] for a full proof. □

Chapter 2

Configuration Spaces

In the previous chapter we have only seen geometric braids on $\mathbb{R}^2$. Geometric braids can be generalized somewhat though. We can look at braid groups on other manifolds. A physical interpretation of this would be points (or particles) moving around on a manifold through time, and tracing their path as a strand. The particles can take up combinations of positions in this manifold, otherwise known as a *configuration*. We call the space of all possible configurations the *configuration space*. One can define it in multiple ways depending on the constraints of the system [6, `Configuration Space (physics)`]. We will define it in a more physically relevant way.

Definition 2.1. *A configuration space of a physical system is the space of all possible configurations of the system.*

In this chapter, we will more formally introduce configuration spaces, and study the braid group and the pure braid group on certain configuration spaces. At the end of this chapter, we will show a proof of an important theorem by Artin.

2.1 Homotopy classes

We will need some topology. I will introduce this along [7]. When considering paths in spaces, one might come across linked loops. For example as seen in Figure 2.1. These linked loops will form the structure we are looking for.

First of all, we need some definitions. Consider the paths B and B', and let them be parameterized by functions $f_0, f_1 : I \to X$ with $I = [0, 1]$. See Figure 2.2 (for now, only pay attention to B and B'). These two paths can be continuously transformed into each other. We call two paths like these *homotopic*.

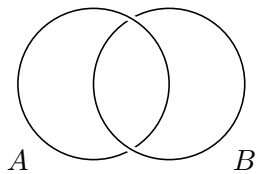

Figure 2.1: Two linked loops in $\mathbb{R}^3$.

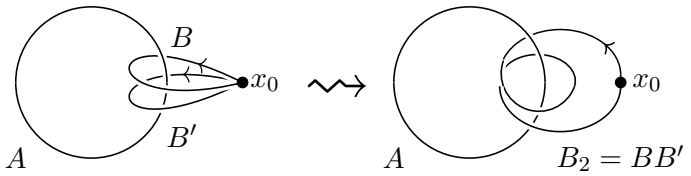

Figure 2.2: Concatenating loops B and B' with base point x_0 in $\mathbb{R}^3 \setminus A$.

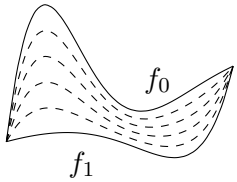

Figure 2.3: Example of what a homotopy of paths looks like. This is an example of a *linear homotopy* $f_t = tf_0 + (1-t)f_1$.

Definition 2.2. *A homotopy of paths in a space X is a family*

$$f_t : I \to X, 0 \leq t \leq 1, \tag{2.1}$$

of continuous functions, such that the following holds.

(i) The endpoints $f_t(0) = x_0$ and $f_t(1) = x_1$ are independent of t.

(ii) The associated map

$$F(s,t) = f_t(s)$$

is continuous.

If two paths f and g are in the same homotopy class, we write $f \simeq g$

It can be proven that homotopy on paths is an equivalence relation. Denote the equivalence class of a path f under homotopy as $[f]$, also known as the *homotopy class* of f. So the paths B and B' will be in the same homotopy class. The paths B and B' are more special though: they are loops. Their starting point x_0 is also their ending point. We call this point x_0 the *base point*.

Homotopies can be determined exactly, but this can become quite cumbersome, and is often left out for the sake of readability.

The structure in equivalence classes of loops comes from concatenating them. We can "add" two loops B, B' through the base point x_0 together by simply concatenating their paths. Let B, B' be parameterized by $f_B, f_{B'} : I \to X$ respectively for some space X. The product of these two paths is

$$f_{BB'} = \begin{cases} f_B(2t) & t \leq \frac{1}{2} \\ f_{B'}(2t-1) & t \geq \frac{1}{2} \end{cases} \tag{2.2}$$

Since we know that $f_B(1) = f_{B'}(0) = x_0$, this product is continuous. When going along the path $B_2 = BB'$, we first traverse B and then B', see Figure 2.2.

Definition 2.3. *In a space X with $x_0 \in X$, let $\pi_1(X, x_0)$ denote the set of homotopy classes of loops in X with base point x_0.*

The set on its own doesn't do much for us, but as mentioned before, there is structure on the loops:

Proposition 2.4. *The set $\pi_1(X, x_0)$ is a group with respect to the product described in equation (2.2): the concatenation of paths.*

Proof Idea. As a representant of the identity homotopy class, consider the constant path

$$f_e : I \to X : t \mapsto x_0.$$

Any path that can be contracted to the constant path f_e is in $[f_e]$. It is clear that concatenating the constant path to any path does not change the old path up to homotopy. Let any loop f_B be given. The inverse of $[f_B]$ will be the homotopy class $[f_B^{-1}]$, represented by

$$f_B^{-1} : I \to X : t \mapsto f_B(1-t).$$

In other words, flipping the direction of the loop f_B. Proving that the concatenation of two loops gives a new loop is fairly straight forward. For a complete proof, see Proposition 1.3 in [7]. □

Notation. *In the future, when we are considering the fundamental group of a space X with respect to an arbitrary point $x_0 \in X$, I will write $\pi_1(X)$ instead of $\pi_1(X, x_0)$ for brevity.*

Example 2.5. *All spaces $\mathbb{R}^n$ (or convex subsets of them) have a trivial fundamental group $\pi_1(\mathbb{R}^n, x_0)$ for any $x_0 \in \mathbb{R}^n$.*

This is because any path f can be contracted to the base point in these spaces, simply by considering the transformation

$$F(s,t) = (1-t)f(s) + tx_0.$$

Example 2.6. *If we consider the space $\overline{A}$ (the setwise complement of A in $\mathbb{R}^3$) in the example given in Figure 2.2, the fundamental group $\pi_1(\overline{A}) \cong \mathbb{Z}$.*

Intuitively, one can see that the fundamental group $\pi_1(\overline{A})$ is generated by B, an element of infinite order.

2.2 Covering Spaces

The concept of *covering spaces* can be useful to find the fundamental group of the spaces they cover. The definition of a covering space is:

Definition 2.7. *A covering space of a space X is a space $\widetilde{X}$ together with a continuous function $p : \widetilde{X} \to X$, such that for each $x \in X$, there exists an open neighborhood U of x for which $p^{-1}(U)$ is a disjoint union of open sets in $\widetilde{X}$. Each of the open sets in this union is homeomorphically mapped onto U by p [7].*

We call such a U *evenly covered*. We call $\tilde{X}$ the *total space*, and X the *base space*. The map p is called the *covering map* and the disjoint open sets in $p^{-1}(U)$ are called *sheets* of $\tilde{X}$ over U.

Note that by this definition, the pullback of p over any x is a discrete fiber.

Proposition 2.8. *Let X be a space, and $p : \widetilde{X} \to X$ a covering map. The pullback $E_x := p^{-1}(x)$ for any $x \in X$ is a discrete subspace of X.*

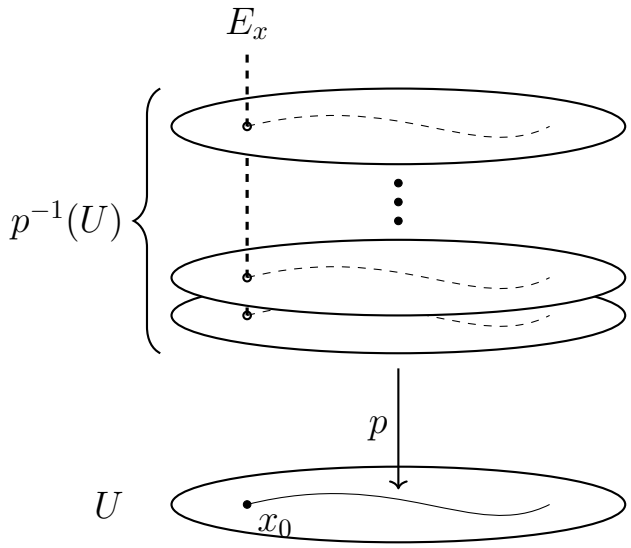

Figure 2.4: Example of a covering space, with pullback of a point x_0 and paths with x_0 as starting point. Image idea from [8, `Covering Space`].

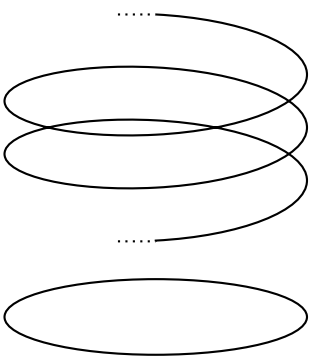

Figure 2.5: Helix as covering space of the circle S^1 [7].

Proof. We will show that for every $\tilde{x} \in E_x$, there is an open neighborhood $\widetilde{U} \subset \tilde{X}$ for which $\widetilde{U} \cap E_x = \{ \tilde{x} \}$.

Note that $\tilde{x}$ is in some sheet of $p^{-1}(U)$. Call this sheet $U_{\tilde{x}}$. We show that $U_{\tilde{x}}$ is the neighborhood we are looking for. Suppose $\tilde{x}' \in E_x \cap U_{\tilde{x}}$. Since $\tilde{x}' \in E_x$, it is also pulled back from x, so $\tilde{x}'$ is also in a sheet $U_{\tilde{x}'}$. Since the sheets of $p^{-1}(U)$ are disjoint, we must have $U_{\tilde{x}'} = U_{\tilde{x}}$. Then because all sheets are mapped homeomorphically to U by p, we must have $\tilde{x}' = \tilde{x}$. □

In fact, one can use this as another, equivalent definition:

Definition 2.7 (Alternative). *A covering space of a space X is a space $\tilde{X}$ together with a continuous function $p : \tilde{X} \to X$ such that for each $x \in X$, there exists an open neighborhood U of x which is evenly covered. This means that the pullback of p over U is isomorphic to a product bundle with discrete fiber $E_x = p^{-1}(x)$. In other words [6, `Covering Space`]:*

$$p^{-1}(U) \cong U \times E_x.$$

We can think of this in a more visual way for clarity, see Figure 2.4. The sheets are depicted as if they are "hovering above" the base space.

Example 2.9. *The real line $\mathbb{R}$ is a covering space of the circle S^1.*

This can be visualized by seeing $\mathbb{R}$ as the helix

$$h : \mathbb{R} \to \mathbb{R}^3 : s \mapsto (\cos 2\pi s, \sin 2\pi s, s), \tag{2.3}$$

see Figure 2.5. The helix projected down onto S^1 is the covering map [7].

2.2.1 Properties of Covering Spaces

Covering spaces have some important properties that we want to use later on, especially regarding homotopy.

Proposition 2.10 (Homotopy Lifting Property)**.** *Let X, Y be topological spaces. Given a covering space $p : \widetilde{X} \to X$, a homotopy $f_t : Y \to X$ and a map $\tilde{f}_0 : Y \to \widetilde{X}$ lifting f_0, then there exists a unique homotopy $\tilde{f}_t : Y \to \tilde{X}$ of $\tilde{f}_0$ that* lifts *f_t, so $p \circ \tilde{f}_t = f_t$.*

We are interested in the case where Y is an interval. In this case, it means that if we have a homotopy of paths in the base space, and a lift in the total space of a path in that homotopy, there is a unique homotopy of paths in the universal space corresponding to the homotopy in the base space. One can think of this visually like in Figure 2.4. If we take a homotopy of paths in the space U, and one corresponding path in any of the sheets, we can find a homotopy of paths in that sheet corresponding to the homotopy in U. For the proof I refer to Proposition 1.30 in [7].

Proposition 2.11 (Path Lifting Property)**.** *Let X, Y be topological spaces, and let $I = [0, 1]$ be the unit interval. Given a covering space $p : \tilde{X} \to X$, a path $f : I \to X$ and $\tilde{x}_0$ a lift of the base point x_0 of f. Then there exists a unique path $\tilde{f} : I \to \widetilde{X}$ lifting f, starting at $\tilde{x}_0$.*

This can be seen as a specific case of the Homotopy Lifting Property, where we take Y to be a point. One can also prove this directly. Proving this for covering spaces of the form $X \times D$ with D a discrete set is fairly straightforward. We can look at the projections

$$\pi_X(\tilde{f}) : I \to X \quad \pi_D(\tilde{f}) : I \to D.$$

Since $\tilde{f}$ is a lift of f, $\pi_X(\tilde{f}) = f$. Note that since I is connected and D discrete, $\pi_D(\tilde{f})$ must be connected, and thus constant. For more complex covering spaces, the proof is more involved, and I point to [6, `Covering Space`], or to Proposition 1.30 in [7].

To finish off these definitions, I will give an example of a use case.

Example 2.12. *The homotopy group $\pi_1(S^1)$ of the circle is the infinite cyclic group generated by the homotopy class of $\omega(s) = (\cos 2\pi s, \sin 2\pi s)$.*

Proof. Consider $\mathbb{R}$ as the helix, from Example 2.9 and Figure 2.5, as covering space $\widetilde{S}^1$ of S^1. The covering map p is the composition of the function h and the projection down on $\mathbb{R}^2$. Let $f : I \to S^1$ be a loop at the base point $x_0 = (1, 0)$, representing an element in $\pi_1(S^1, x_0)$. By the Path Lifting Property there is a unique lifted path $\tilde{f}$ in $\mathbb{R}$ starting at 0. This path $\tilde{f}$ ends at an integer n, since $p^{-1}(x_0) = \mathbb{Z} \subset \mathbb{R}$.

We can define specific paths on the circle, winding around it n times:

$$\omega_n : I \to S^1 : s \mapsto (\cos 2\pi ns, \sin 2\pi ns).$$

Note that

$$[\omega_n] = [\omega]^n.$$

Lifting this path to $\mathbb{R}$ gives:

$$\tilde{\omega}_n(s) = ns.$$

So $\tilde{f}$ and $\tilde{\omega}_n$ are in the same homotopy class.

For uniqueness of n, suppose that $f \simeq \omega_n$ and $f \simeq \omega_m$. Then $\omega_n \simeq \omega_m$. By the Homotopy Lifting Property, this homotopy lifts to a homotopy in $\widetilde{S^1}$. So $\tilde{\omega}_n \simeq \tilde{\omega}_m$. However, the endpoints for all paths in a homotopy class must be equal. The endpoint of $\tilde{\omega}_n$ is n, and that of $\tilde{\omega}_m$ is m, so $n = m$. [7] □

Another important concept related to covering spaces is the group of *covering transformations* or *deck transformations*.

Definition 2.13. *For a space $\widetilde{X}$ covering X, the group* $\mathrm{deck}(\widetilde{X})$ *of deck transformations is the group of automorphisms f on $\widetilde{X}$ such that p is invariant under composition with f, or in other words [6,* `Deck Transformation`*]*

$$\mathrm{deck}(\widetilde{X}) := \left\{ f \;\middle|\; f \in \mathrm{Aut}(\widetilde{X}), p \circ f = p \right\}$$

2.3 Configuration spaces

I will stick to the notation used by [9], when talking about configuration spaces. Let M be a manifold. Call the amount of points we are observing N. Naively, one might say that the configuration space would be M^N. However, we do not want particles to be occupying the same position in space (hard-core model). So we remove the diagonal points. Define

$$\Delta := \left\{ (z_1, z_2, \ldots, z_N) \subset M^N \;\middle|\; z_i = z_j \text{ for any } i \neq j, 1 \leq i, j \leq N \right\} \tag{2.4}$$

We call the configuration space for N *distinguishable particles*

$$F_N(M) := M^N \setminus \Delta. \tag{2.5}$$

What it means for particles to be distinguishable is essentially the following: the configuration (z_1, z_2) is not the same as the configuration (z_2, z_1) for $z_1 \neq z_2 \in M$. For *indistinguishable particles*, these 2 configurations are the same, and we need to divide out the action of the symmetric group S_N for N particles to remove these. Define

$$Q_N(M) := (M^N \setminus \Delta)/S_N \tag{2.6}$$

to be the configuration space of N indistinguishable particles, or the *orbit space* of M [9, Section 2.1]. See Figure 2.6 for a visual example. The pure braid group on the manifold M is the fundamental group of the space $F_N(M)$, $\pi_1(F_N(M))$. The (full) braid group on the manifold M is the fundamental group $\pi_1(Q_N(M))$.

Lemma 2.14. *The natural map*

$$\mathfrak{p} : F_N(M) \to Q_N(M) \tag{2.7}$$

is a covering map. In fact, it is a regular covering space projection*, meaning that*

$$\pi_1(F_N(M)) \trianglelefteq \pi_1(Q_N(M)) \tag{2.8}$$

Proof. This is an application of Proposition 1.40 in [7], and mentioned explicitly as Proposition 1.1 in [5]. □

The configuration spaces of some specific spaces can be found [4].

2.4 Braid Groups on Manifolds

As mentioned, the configuration spaces for some specific spaces can be found exactly. We will look at a few, along [4], where a nice technique is used to find these.

2.4.1 The Strategy

Let us consider N particles, moving around on a manifold $M = \mathbb{R}^n$. Call the coordinates of these particles x_i with $i = 1, 2, \ldots, N$. We can consider these particles separately, but we can simplify the problem slightly by looking at the center of mass coordinate, and the relative positions of the particles. The center of mass (c.m.) coordinate

$$x_{\text{cm}} = N^{-1} \sum_{i=1}^{N} x_i \tag{2.9}$$

Note that the center of mass does not change under permutation of the particles and $x_{\text{cm}} \in \mathbb{R}^n$. This means that the N particle configuration space is a product

$$Q_N(\mathbb{R}^n) = \mathbb{R}^n \times r(n, N), \tag{2.10}$$

of the c.m. coordinate space, and a relative space $r(n, N)$, representing the $(N-1)n$ degrees of freedom of the particles relative to each other [4]. This is mostly a physical argument, but we can give a more formal argument to show that this splitting holds.

The formal argument would be to look at the action of $\mathbb{R}^n$ as group under addition on $Q_N(\mathbb{R}^n)$. We can divide out this action to obtain the space $Q_N(\mathbb{R}^n)/\mathbb{R}^n$. As a representant of points in this quotient space, we can in fact choose the configurations where the center of mass is at the origin.

Lemma 2.15. *The space $Q_N(\mathbb{R}^n)$ for $N, n \in \mathbb{Z}_{>0}$ splits as*

$$Q_N(\mathbb{R}^n) = \mathbb{R}^n \times r(n, N). \tag{2.11}$$

where $r(n, N)$ is a space dependent on n and N.

Proof. We claim that

$$Q_N(\mathbb{R}^n) \cong \mathbb{R}^n \times \left(Q_N(\mathbb{R}^n)/\mathbb{R}^n\right).$$

We can find a map

$$f : Q_N(\mathbb{R}^n) \to \mathbb{R}^n \times \left(Q_N(\mathbb{R}^n)/\mathbb{R}^n\right)$$

by setting

$$f(q) = (\text{CM}(q), [q])$$

where $[q]$ is the equivalence class of q under the action of $\mathbb{R}^n$, and we call the map taking a configuration to its center of mass

$$\text{CM} : Q_N(\mathbb{R}^n) \to \mathbb{R}^n,$$

as defined in (2.9). Note that we can also define CM in the exact same way on $\mathbb{R}^n$ or $F_N(\mathbb{R}^n)$.

One can prove injectivity and surjectivity for f fairly simply to show it is bijective. I will leave this as an exercise to the reader.

We will show that the map CM is open and continuous. Continuity is more clear when looking at CM as if its domain was $(\mathbb{R}^n)^N$. This map is obviously continuous. Then the restriction to $F_N(\mathbb{R}^n)$ is also continuous, and since it is invariant under symmetry of S_N, it is continuous on $Q_N(\mathbb{R}^n)$.

We can verify openness of CM by considering an open ball $B(q;\epsilon) \subset F_N(\mathbb{R}^n)$ (note, not Q_N) around a configuration q, with radius ϵ. From the way the topology on $F_N(\mathbb{R}^n)$ is induced, we can find open balls $B_i \subset F_N(\mathbb{R}^n)$ of radius ϵ_i around the points x_i in the configuration $q = (x_1, \ldots, x_N)$ such that

$$B_1 \times B_2 \times \ldots \times B_N \subset B(q;\epsilon).$$

We can then shift the configuration by any $x \in \mathbb{R}^n$ with $||x|| < \delta := \min_{i=1,\ldots,N} \epsilon_i$. With this, we see that there is a ball of radius δ around x_0 in the image of CM of $B(q;\epsilon)$. Since open sets in $Q_N(\mathbb{R}^n)$ correspond to open sets in $F_N(\mathbb{R}^n)$, this verifies that CM is open on $Q_N(\mathbb{R}^n)$.

The map sending q to $[q]$ is continuous by definition. To see that it is open, take an open set $U \subset Q_N$ and consider its image

$$\{\, [q] \mid q \in U \,\} \subset Q_N(\mathbb{R}^n)/\mathbb{R}^n.$$

The preimage of this set under the quotient map is

$$\left\{\, q' \;\middle|\; q' \in [q], q \in U \,\right\} = \{\, x + q \mid x \in \mathbb{R}^n, q \in U \,\} = \bigcup_{x \in \mathbb{R}^n} x + U$$

which is a union of open sets, and thus an open set. Therefore, the map taking q to $[q]$ is open.

Because of this, f is open, continuous and bijective, so it is a homeomorphism, and thus

$$Q_N(\mathbb{R}^n) \cong \mathbb{R}^n \times (Q_N(\mathbb{R}^n)/\mathbb{R}^n)\,,$$

as desired. □

Note that the physical argument for splitting the configuration space does not work for general subspaces of $\mathbb{R}^n$, but only for convex subspaces. If the subspace is not convex, the c.m. coordinate might not lie in the original subspace, for example consider the circle S^1 in 2 dimensions: two particles on opposite sides would have their center of mass in the middle of the circle, which is not part of S^1.

2.4.2 Two Particle Systems

The simplest (non-trivial) case we can consider is that of two particle systems. In this case, the relative space $r(n,2)$ comes from identifying

$$x_{\text{rel}} = x_1 - x_2 \text{ and } x_2 - x_1 = -x_{\text{rel}} \tag{2.12}$$

in $\mathbb{R}^n \setminus \{\, 0 \,\}$, as the result of the action of S_2. As an illustration: for distinguishable particles, the relative space would be $\mathbb{R}^n \setminus 0$. Since the particles may not take up the same position, 0 must be excluded. Then in this system, exchanging the 2 particles (or: flipping the sign of the relative position) must be identified as the same configuration.

This leads to the relative space being

$$r(n,2) = (0,\infty) \times \mathbb{P}_{n-1}. \tag{2.13}$$

Where $(0,\infty)$ is the length of x_{rel}, and $\mathbb{P}_{n-1}$, the *real projective space* of dimension $n-1$, the direction.

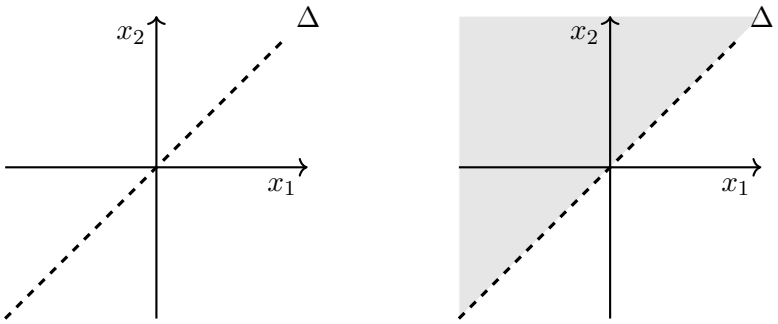

Figure 2.6: An illustration of the configuration space $F_2(\mathbb{R})$ of 2 distinguishable particles in $\mathbb{R}$ on the left, and $Q_2(\mathbb{R})$ for indistinguishable particles is the non-shaded region on the right.

Definition 2.16. *The* real projective space *of dimension n, denoted by $\mathbb{P}_n$, is given by*

$$\mathbb{P}_n = (\mathbb{R}^{n+1} \setminus \{ 0 \})/\mathbb{G} \tag{2.14}$$

where $\mathbb{G}$ is the equivalence relation

$$x \mathbb{G} y \iff x = \lambda y$$

for any $\lambda \in \mathbb{R}$ [6, `Projective Space`].

Note. *The real projective space of dimensions n can also be found by identifying antipodal points in the n-dimensional sphere S^n.*

One can think of the space $\mathbb{P}_n$ as the space of all lines through the origin in $\mathbb{R}^{n+1}$, or as all "directions" in $\mathbb{R}^{n+1}$. The projective space $\mathbb{P}_0$ is a point, and $\mathbb{P}_1$ is homemophic to a circle [4].

Along The Line

The simplest case would be when particles move along a line. Of course, this problem is much less relevant, since with a hard core model, paricles cannot exchange positions at all along a 1D space. However, it can be useful to see what the configuration space is for two particles on a line, just to get a bit of a feeling for it.

Since $\mathbb{P}_0$ is a point, we have $r(1,2) \cong (0,\infty)$. Then the configuration space will be the open half plane

$$Q_2(\mathbb{R}) = \mathbb{R} \times (0,\infty), \tag{2.15}$$

see Figure 2.6. It can be noted that the fundamental group $\pi_1(Q_2(\mathbb{R}))$ is trivial, since every path can be contracted to a point.

In The Plane

A more advanced case is when we look at 2 particles in the plane. In this case, particles *can* exchange positions. The relative space $r(2,2)$ is the plane $\mathbb{R}^2 \setminus \{ 0 \}$ with opposing points identified. One can view this as the plane cut along a half line in the origin, and then wrapping it around into a cone. The resulting cone can then be flattened into $\mathbb{R}^2 \setminus \{ 0 \}$ again.

There are two types of loops in this space $r(2,2)$: those that loop around the singularity and those that don't. There are two major differences about these paths in $r(2,2)$. The most obvious difference is that loops around the singularity cannot be contracted to a point, whereas the other type of loops can.

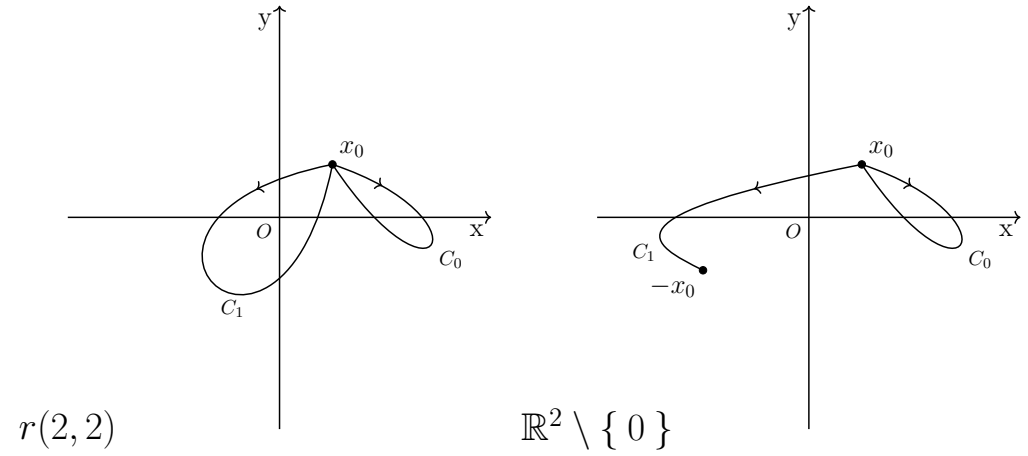

Figure 2.7: The relative space $r(2,2)$ and the covering space $\mathbb{R}^2 \setminus \{ 0 \}$. Two paths C_0 and C_1 are drawn, along with their lifts in $\mathbb{R}^2 \setminus \{ 0 \}$.

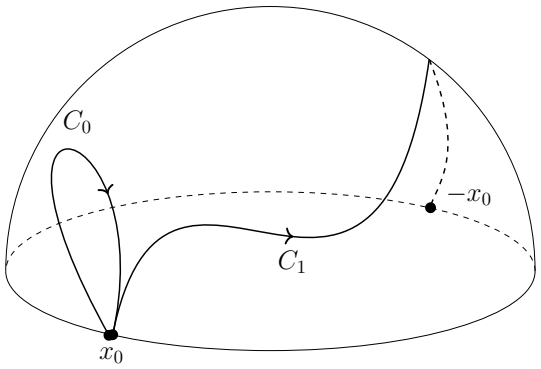

Figure 2.8: The projective plane $\mathbb{P}_2$ with two loops C_0 and C_1.

The second difference is that loops around the singularity are in fact not loops in the covering space $\mathbb{R}^2 \setminus \{ 0 \}$ of $r(2,2)$ (note that this is not the only possible covering space, just a covering space). The lifts of loops around the singularity are in fact paths starting at x_0 and ending at $-x_0$. This follows from the Path Lifting Property.

The fundamental group of this space is $\mathbb{Z}$, this can be derived much like we did for the circle in Example 2.12. We can also derive it using the following lemma:

Lemma 2.17. *For two spaces X and Y, the fundamental group $\pi_1(X \times Y)$ is isomorphic to $\pi_1(X) \times \pi_1(Y)$ if X and Y are path connected.*

This lemma corresponds with Proposition 1.12 from [7]. With this we can easily see that

$$\pi_1(Q_2(\mathbb{R}^2)) = \pi_1(\mathbb{R}^2 \times \mathbb{P}_1 \times (0,\infty)) = \pi_1(\mathbb{P}_1) = \pi_1(S^1) = \mathbb{Z}, \tag{2.16}$$

since all of these spaces are path connected, both $\mathbb{R}^2$ and $(0,\infty)$ have a trivial fundamental group, and $\mathbb{P}_1$ is the circle, as mentioned before. Not coincidentally, $B_2 \cong \mathbb{Z}$.

In $\mathbb{R}^3$

Perhaps the most physically relevant case is that of particles in $\mathbb{R}^3$. Using the same strategy, we know that

$$r(3,2) = (0,\infty) \times \mathbb{P}_2.$$

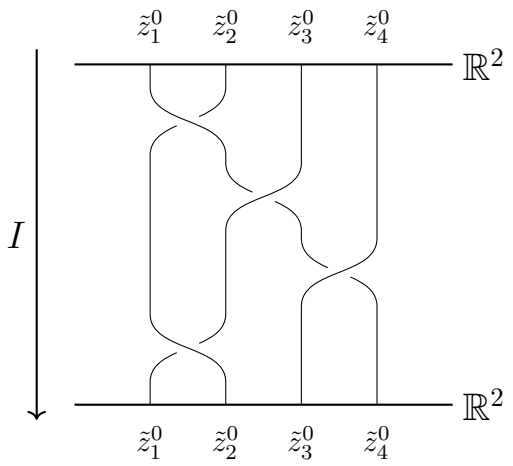

Figure 2.9: A loop in Q_4 with base point z^0, lifted to a path in F_4 with starting point $\tilde{z^0}$, depicted as separate paths in $\mathbb{R}^2 \times I$.

Now, we are then most interested in the space $\mathbb{P}_2$. This space is the sphere S^2 with antipodal points associated, as noted before. Another way of representing it is as the hemisphere with opposing equatorial points associated, see Figure 2.8. Note that the path C_1 is in fact a loop, since in $\mathbb{P}_2$, the point $-x_0$ is the same point as x_0.

It might seem as if C_1 is contractible to x_0, but it is not. To see this, consider the sphere S^2 as covering space of $\mathbb{P}_2$, with the quotient map induced by $\mathbb{G}$ from Definition 2.16 as covering map. The lift $\widetilde{C}_1 \subset S^2$ of C_1 then starts at x_0 and ends at $-x_0$. If C_1 were contractible to a point, $\widetilde{C}_1$ must be as well, because of the Homotopy Lifting Property. However, in a homotopy class, the endpoints of all paths are the same, so $\widetilde{C}_1$ cannot be contracted to a point! Moving along C_1 twice gives the lift $\widetilde{C}_1^2$, which is contractible to a point in S^2, and induces a homotopy to contract $\widetilde{C}_1^2$ to a point. The fundamental group for this space is then the group of two elements, $\mathbb{Z}_2$. Using the same reasoning as for equation (2.16), we find that

$$\pi_1(Q_2(\mathbb{R}^3)) = \mathbb{Z}_2 \tag{2.17}$$

In fact, for $\mathbb{R}^3$, one can derive that [9, Section 2.4.4]

$$\pi_1(Q_N(\mathbb{R}^3)) = S_N, \tag{2.18}$$

and indeed $S_2 \cong \mathbb{Z}_2$.

2.5 The Braid Group on the Plane

In the previous section, we saw that the braid group on two strands arises as fundamental group of the configuration space of two indistinguishable particles in $\mathbb{R}^2$. However, we can prove that in fact, B_N arises as the fundamental group of the configuration space of N indistinguishable particles in $\mathbb{R}^2$. The proof by Fadell and Van Buskirk will be presented, as given by Birman in [5, Section 1.4].

Notation. *Since we will be talking about $F_N(\mathbb{R}^2)$ and $Q_N(\mathbb{R}^2)$ a lot, We will abbreviate them to F_N and Q_N, just for this section.*

First of all, let us get an idea of what elements in Q_N look like. Recall the covering projection $\mathfrak{p}$ from Lemma 2.14. Choose a base point

$$\tilde{z}^0 = (\tilde{z}_1^0, \ldots, \tilde{z}_N^0) \in F_N,$$

which corresponds to a unique point

$$z_0 = \mathfrak{p}(\tilde{z}^0) \in Q_N.$$

We can represent an element in $\pi_1(Q_N)$ with a loop

$$l : I \to Q_N$$

with $l(0) = l(1) = z_0$. This path lifts to a unique path

$$\tilde{l} : I \to F_N$$

with $\tilde{l}(0) = \tilde{z}_0$ and $\mathfrak{p}(\tilde{l}(1)) = z^0$. This lifted path defines a tuple of paths in $\mathbb{R}^2$, since

$$\tilde{l}(t) = (\tilde{l}_1(t), \tilde{l}_2(t), \ldots, \tilde{l}_N(t))$$

with $\tilde{l}_i(t) \in \mathbb{R}^2$. These arcs never intersect at any $t \in I$, by the definition of $F_N(M)$. This gives us exactly the geometric braids we have seen in chapter 1! See Figure 2.9 for a representation in this way. Thinking of the diagrams this way, one might notice that the pure braids then correspond to $\pi_1(F_N)$.

An important lemma used in the proof by Fadell and Van Buskirk is the *five lemma*. We only really need a specific case of this, the *short five lemma*, in the context of groups, given below.

Definition 2.18 (Short Exact Sequence)**.** *A sequence of objects A, B, C with homomorphisms p and q, as given in the diagram below*

$$\{\,1\,\} \longrightarrow A \xrightarrow{\ p\ } B \xrightarrow{\ q\ } C \longrightarrow \{\,1\,\}$$

is called a short exact sequence *if $p(A) = \ker q$.*

Lemma 2.19 (Short Five Lemma)**.** *Let A, B, C, A', B', C' be objects in a commuting diagram*

$$\begin{array}{ccccccccc} \{\,1\,\} & \longrightarrow & A & \xrightarrow{\ p\ } & B & \xrightarrow{\ q\ } & C & \longrightarrow & \{\,1\,\} \\ & & \downarrow{\scriptstyle g} & & \downarrow{\scriptstyle f} & & \downarrow{\scriptstyle h} & & \\ \{\,1\,\} & \longrightarrow & A' & \xrightarrow{\ p'\ } & B' & \xrightarrow{\ q'\ } & C' & \longrightarrow & \{\,1\,\} \end{array}$$

where p, q, p', q', g, f, h are homomorphisms and $\{\,1\,\}$ is the trivial group. If the rows are short exact sequences (i.e., $p(A) = \ker q$ and $p'(A') = \ker q'$), and g and h are isomorphisms, then f is also an isomorphism.

A proof of this lemma can be found in many books on algebra, or on nLab for example.

We still need some additional work for the main theorem of this section. Let $H_m = \{\, h_1, \ldots, h_m \,\}$ be a set of m distinct points in $\mathbb{R}^2$. Define $F_{m,N}$ to be the space

$$F_{m,N} = F_N(\mathbb{R}^2 \setminus H_m), \tag{2.19}$$

the configuration space of N distinguishable particles on the *m-punctured plane*. Note that $F_N = F_{0,N}$. The main result we need about the spaces $F_{m,N}$ is a theorem for which I will present the proof in Appendix A:

Theorem 2.20. *There exist homomorphisms ι_* and π_* such that the following sequence of groups is exact:*

$$\{\,1\,\} \longrightarrow \pi_1(F_{N-1,1}) \xrightarrow{\ \iota_*\ } \pi_1(F_N) \xrightarrow{\ \pi_*\ } \pi_1(F_{N-1}) \longrightarrow \{\,1\,\}$$

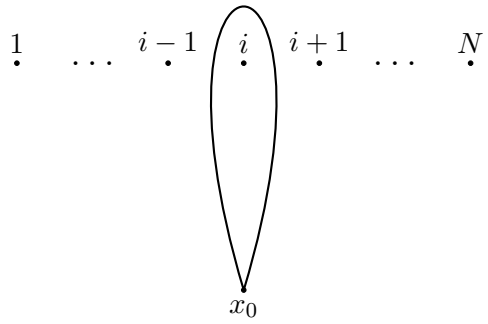

Figure 2.10: The i-th generator of the fundamental group of the N-punctured plane $F_{N,1}$

Note. *Since $F_{N-1,1}$ is the configuration space of 1 particle on the $N-1$-punctured plane, and is in fact simply the space $\mathbb{R}^2 - H_{N-1}$, the fundamental group $\pi_1(F_{N-1,1})$ is the free group on $N-1$ generators, $\mathcal{F}_{N-1}$. Every generator is a loop around precisely one puncture, see Figure 2.10.*

Now we are ready for the main theorem of this section.

Theorem 2.21 (Artin, 1925)**.** *The group $\pi_1(Q_N)$ admits a presentation with generators $\sigma_1, \ldots, \sigma_{n-1}$ and defining relations* (B1) *and* (B2)*.*

Proof. The plan for this proof is to first reduce our problem to the space F_N, and only looking at pure braids. We can then inductively prove the result.

As before, we denote the abstract representation of the braid group on N strands by B_N, as in Definition 1.1. For elements in $\pi_1(Q_N)$, we write $\overline{\sigma}_1, \ldots, \overline{\sigma}_{N-1}$. We have seen visual representations of these in terms of braid diagrams, as discussed in the above paragraph. We can define

$$\mathfrak{i} : B_N \to \pi_1(Q_N) : \sigma_i \mapsto \overline{\sigma}_i$$

for $i = 1, 2, \ldots, N-1$. One can verify pictorially that the $\overline{\sigma}_i$ satisfy the braid relations (see Figure 1.2 for example). For a rigorous proof, see [1, Section 1.2]. We can then apply Lemma 1.2 to see that $\mathfrak{i}$ is indeed a homomorphism.

Recall the map $\mathfrak{p} : F_N \to Q_N$ from Lemma 2.14. We can make our visual representation of $\pi_1(Q_N)$ a bit more precise by taking

$$\tilde{z}^0 = ((1,0),(2,0),\ldots,(n,0)) \quad \text{and} \quad z^0 = \mathfrak{p}(\tilde{z}^0)$$

and taking the path of the generator $\overline{\sigma}_i$ in $F_N(\mathbb{R}^2)$ to be

$$\tilde{l}(t) = \Big((1,0),\ldots,(i-1,0),\ \tilde{l}_i(t),\ \tilde{l}_{i+1}(t),\ (i+2,0),\ldots,(n,0)\Big)$$

with

$$\tilde{l}_i(t) = (i+t, -\sqrt{t-t^2}) \quad \text{and} \quad \tilde{l}_{i+1}(t) = (i+1-t, \sqrt{t-t^2}).$$

This is nothing more than a more precise definition of the generators as seen in braid diagrams.

We then construct a homomorphism

$$\overline{\nu} : \pi_1(Q_N) \to S_N, \tag{2.20}$$

as follows: let $a \in \pi_1(Q_N)$ be a loop in Q_N with base point z^0, and let $\tilde{a}$ be the uniquely lifted path of this loop, with starting point $\tilde{z}^0$. Define

$$\overline{\nu}(a) = \begin{pmatrix} \tilde{a}_1(0), \ldots, \tilde{a}_N(0) \\ \tilde{a}_1(1), \ldots, \tilde{a}_N(1) \end{pmatrix} \in S_N. \tag{2.21}$$

Essentially, we send the path a to the permutation exchanging the endpoints of the lifted path $\tilde{a}$, in the same sort of way we did in equation 1.1.

We want to verify that $\overline{\nu}$ is indeed a homomorphism. Visually, one can see this as pasting two braid diagrams after another, and following the new strands to find the new permutation. We can give a more strict argument though. Let a, a' be two loops in $\pi_1(Q_N)$. We wish to show that $\overline{\nu}(aa') = \overline{\nu}(a)\overline{\nu}(a')$.

For this, first lift a to a path $\tilde{a}$ in F_N, starting at $\tilde{z}^0$. Then $\tilde{a}$ permutes the coordinates of $\tilde{z}^0$ by $\overline{\nu}(a)$. Call this permutation τ. The ending point of $\tilde{a}$ is $\tau\tilde{z}^0$, which is the point $\tilde{z}^0$ with its coordinates permuted by τ.

Lift a' to a path $\tilde{a}'_\tau$ in F_N, starting at $\tau\tilde{z}^0$. Note that the concatenation $\tilde{a}\tilde{a}'_\tau$ is the unique lift of aa', starting at $\tilde{z}^0$. Since the starting point of $\tilde{a}'_\tau$ is $\tilde{z}^0$ permuted by τ, we can also write $\tilde{a}'_\tau$ as $\tau\tilde{a}'$, where $\tilde{a}'$ is the path lifted from a' starting at $\tilde{z}^0$ itself. As a braid diagram, the path $\tau\tilde{a}'$ would look the same, as merely the indices of the strands are permuted. The resulting permutation of $\tau\tilde{a}'$ would then be $\tau\overline{\nu}(a')$, as expected.

We can determine the kernel of $\overline{\nu}$ as well: if for every $i = 1, 2, \ldots, N-1$, we have $\tilde{a}_i(1) = \tilde{a}_i(0)$, we find a loop in $\pi_1(F_N)$, and vice versa, for every loop $\tilde{a}$ in $\pi_1(F_N)$, we have $\tilde{a}_i(1) = \tilde{a}_i(0)$. The kernel of $\overline{\nu}$ is the pure braid group $\pi_1(F_N)$.

We can take the homomorphism from Equation (1.1) as corresponding homomorphism

$$\nu : B_N \to S_N : \sigma_i \mapsto (i, i+1)$$

for $i = 1, 2, \ldots, N-1$. As in Chapter 1, we take $P_N = \ker \nu$. Using this homomorphism, we can reduce our problem to a simpler case.

Lemma 2.22. *The homomorphism $\mathfrak{i} : B_N \to \pi_1(Q_N)$ is an isomorphism if $\mathfrak{i}\big|_{P_N}$ is an isomorphism onto $\pi_1(F_N)$.*

Proof. Recall from Lemma 2.14 that

$$\pi_1(F_N) \trianglelefteq \pi_1(Q_N),$$

which in this case also follows from $\pi_1(F_N) = \ker(\overline{\nu})$. We can then naturally include $\pi_1(F_N)$ in $\pi_1(Q_N)$. This gives rise to the commutative diagram

$$\begin{array}{ccccccccc} \{1\} & \longrightarrow & P_N & \xrightarrow{\text{id}} & B_N & \xrightarrow{\nu} & S_N & \longrightarrow & \{1\} \\ & & \downarrow{\scriptstyle \mathfrak{i}|_{P_N}} & & \downarrow{\scriptstyle \mathfrak{i}} & & \downarrow{\scriptstyle \text{id}} & & \\ \{1\} & \longrightarrow & \pi_1(F_N) & \xrightarrow{\text{id}} & \pi_1(Q_N) & \xrightarrow{\overline{\nu}} & S_N & \longrightarrow & \{1\} \end{array}$$

One can easily verify that the rows are exact sequences. Since the identity mapping is an isomorphism, $\pi_1(F_N) = \ker \overline{\nu}$, and $P_N = \ker(\nu)$ by definition. The Short Five Lemma tells us the lemma holds. □

We are then left to prove the premise of this lemma. The idea is to do this by induction on N. Take P_N to be the group generated by the generators

$$A_{i,j} \quad 1 \leq i < j \leq N$$

as in Theorem 1.5. Also recall the group U_n from the proof of this theorem, defined as

$$U_N = \ker f_N,$$

where $f_N : P_N \to P_{N-1}$ is the *forgetting homomorphism*. Corresponding to this homomorphism, we have the homomorphism

$$\pi_* : \pi_1(F_N) \to \pi_1(F_{N-1}) \tag{2.22}$$

from Theorem 2.20. With these groups we can construct a commutative diagram as follows:

$$\begin{array}{ccccccccc}
\{\,1\,\} & \longrightarrow & U_N & \xrightarrow{\mathrm{id}} & P_N & \xrightarrow{f_N} & P_{N-1} & \longrightarrow & \{\,1\,\} \\
 & & \downarrow{\scriptstyle \mathfrak{i}|_{U_N}} & & \downarrow{\scriptstyle \mathfrak{i}|_{P_N}} & & \downarrow{\scriptstyle \mathfrak{i}|_{P_{N-1}}} & & \\
\{\,1\,\} & \longrightarrow & \pi_1(F_{N-1,1}) & \xrightarrow{\iota_*} & \pi_1(F_N) & \xrightarrow{\pi_*} & \pi_1(F_{N-1}) & \longrightarrow & \{\,1\,\}
\end{array}$$

Here, ι_* is the corresponding homomorphism in Theorem 2.20. In the proof idea for Theorem 1.5, we mentioned that U_N is free on the generators $A_{i,N} \in P_N$. A proof of this can be found in [1, Theorem 1.16]. From the definition of the $A_{i,j}$, and the way we defined elements in $\pi_1(F_N)$, the image $\mathfrak{i}(A_{j,N})$ may be represented by a loop based at z_N^0, encircling z_j^0 once, cutting it off from the rest of the points z_i^0 with $i \neq j$ (see also Figure 1.4).

Taking $F_{N-1,1}$ to be $F_1(\mathbb{R}^2 \setminus \{\, z_1^0, \ldots, z_{N-1}^0 \,\})$ and z_N^0 as base point for $\pi_1(F_{N-1,1})$ makes it so

$$\{\, \mathfrak{i}(A_{j,N}) \mid 1 \leq j \leq N-1 \,\}$$

is a basis for $\pi_1(F_{N-1,1})$. With this, we have found that $\mathfrak{i}|_{U_N}$ is an isomorphism from U_N to $\pi_1(F_{N-1,1})$, since both are the free group on $N-1$ generators.

Note that P_1 is the trivial group, and so is F_1. Thus, $\mathfrak{i}|_{P_1}$ is an isomorphism, and using the five lemma, we can then conclude that by induction, $\mathfrak{i}|_{P_N}$ is an isomorphism for all N. □

Chapter 3

Other Representations

Besides the algebraic representation we initially introduced, and the braid group as fundamental group of the space $Q_N(\mathbb{R}^2)$ we saw in Section 2.5, there are other representations of the braid group B_n. In this chapter we are going to explore a few of these. Firstly the braid group represented by self-homeomorphisms on the punctured disk, then the Burau representation and finally the Lawrence-Krammer-Bigelow representation.

3.1 The Punctured Disk

Another way to represent the braid group is by considering the action of *Dehn half-twists* on the fundamental group of the punctured disk. Fix a set H_n of n distinct points $h_1, \ldots, h_n$ in the interior of the unit disk D, and take d_0 to be a point on the boundary of D. Like mentioned before about the n-punctured plane, the fundamental group of the n-punctured disk

$$D_n = D \setminus H_n$$

is the free group on n generators $\mathcal{F}_n$. See Figure 3.1 for a representation of the i-th generator, which we call x_i.

Perhaps the most interesting part of this representation is seeing how generators $\sigma_i \in B_n$ can be represented as actions on this group. We can do this by representing them as *Dehn half-twist*s [10].

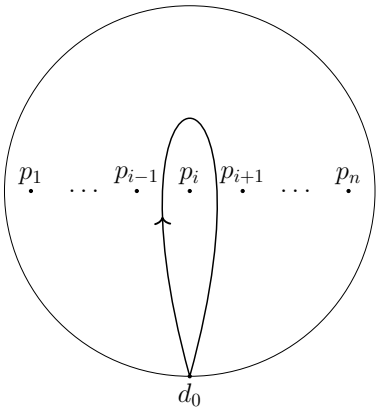

Figure 3.1: The i-th generator x_i of the fundamental group of the n-punctured disk D_n

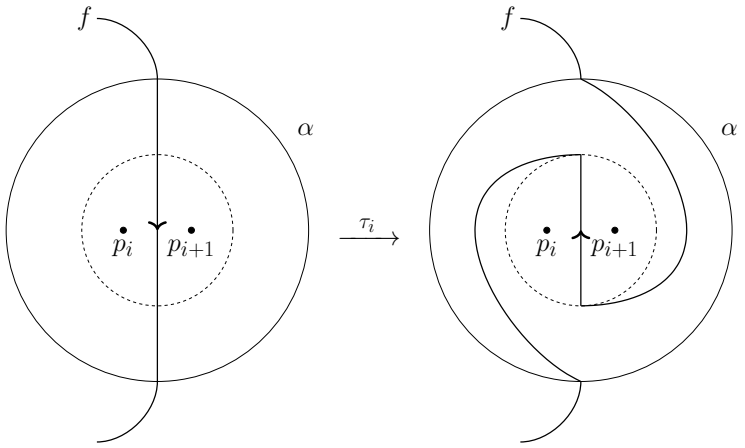

Figure 3.2: The Dehn half-twist τ_i. If one thinks of the path f as being closed on the bottom, not encircling any of the other punctures, like in Figure 3.1, this diagram in fact shows relation (3.2).

Definition 3.1. *Consider a loop α enclosing the punctures p_i and p_{i+1}, and identify its interior with the twice-punctured disk $D_2 = D \setminus \{ -\frac{1}{4}, \frac{1}{4} \}$. In D_2, define the annulus*

$$A = \left\{ z \in D_2 \;\middle|\; \frac{1}{2} \leq |z| \leq 1 \right\}.$$

We define the Dehn half-twist τ_i is for $(s,t) \in \left(S^1 \times I\right) \setminus \{ -\frac{1}{4}, \frac{1}{4} \}$. We associate a point $te^{i\theta} \in D$ with (s,t) for $s = e^{i\theta}$. Then τ_i is defined as

$$\tau_i(s,t) = \begin{cases} (e^{-\pi i t}s, t) & \text{if } (s,t) \in A \\ (-s,t) & \text{otherwise} \end{cases}, \tag{3.1}$$

also seen in Figure 3.2. Note that if we extend the domain to D, the holes would be mapped to each other.

By drawing diagrams, we can verify that

$$\tau_i x_i = x_i x_{i+1} x_i^{-1} \tag{3.2}$$

$$\tau_i x_{i+1} = x_i \tag{3.3}$$

$$\tau_i x_j = x_j \qquad j \neq i, i+1, \tag{3.4}$$

where $\tau_i x_j$ means applying $(\tau_i)_*$ to the loop $x_j \in \pi_1(D_n)$, where $(\tau_i)_*$ is the induced homomorphism $\pi_1(D_n) \to \pi_1(D_n)$. Relation (3.2) can be seen in Figure 3.2. How one comes from $x_i x_{i+1} x_i^{-1}$ to the path in Figure 3.2 can be seen in Figure 3.3. If one takes the ends of the path f outside of α to go the other way, and f to be closed on the right side of α, not encircling any other punctures, this verifies relation (3.3). Relation (3.4) is trivial.

With these relations, it can easily be verified that

$$\tau_i \tau_{i+1} \tau_i = \tau_{i+1} \tau_i \tau_{i+1} \quad \text{and} \quad \tau_i \tau_j = \tau_j \tau_i \tag{3.5}$$

for $i, j = 1, 2, \ldots, n-1$ and $|i-j| \geq 2$, as actions on $\pi_1(D_n, d_0)$. In other words, the τ_i satisfy the braid relations (B1) and (B2). We can then, using Lemma 1.2, construct a simple homomorphism from $B_n \to \mathrm{Aut}(\pi_1(D_n, d_0))$, the group of *automorphisms* on $\pi_1(D_n, d_0)$, by mapping σ_i to τ_i.

One can construct the inverse of this homomorphism on its image by "walking along" the loops in $\pi_1(D_n, d_0)$ through time, and plotting them as geometric braids, restricted to D instead of $\mathbb{R}^2$, as Jackson shows in [10].

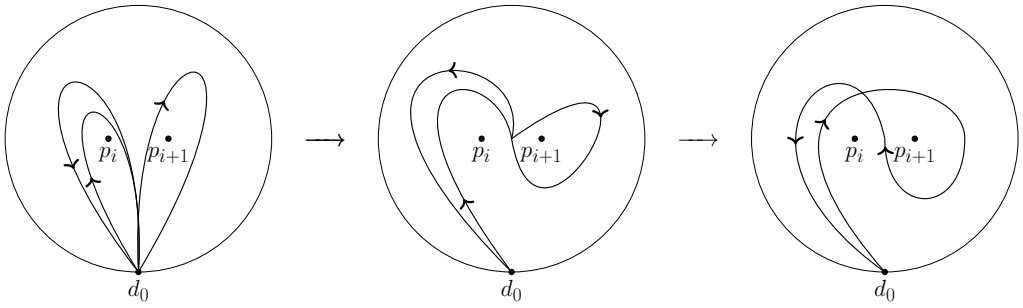

Figure 3.3: The element $x_i x_{i+1} x_i^{-1} \in \pi_1(D_n, d_0)$, the right hand side of Equation (3.2). Only two (neighboring) punctures are shown for simplicity. By isolating a circle around p_i and p_{i+1} in the rightmost image, one essentially retrieves the right hand side of Figure 3.2.

These homomorphisms give rise to the following theorem.

Theorem 3.2. *The homomorphism $\sigma_i \mapsto \tau_i$ gives a* faithful representation *of B_n as a group of automorphisms of the free group $\mathcal{F}_n$.*

Here, *faithful* simply means that the homomorphism is injective, or equivalently, that the homomorphism has a trivial kernel. In fact, one can prove the following:

Theorem 3.3. *B_n is isomorphic to the subgroup of automorphisms of $\pi_1(D_n, d_0) = \mathcal{F}_n$ induced by homeomorphisms $D_n \to D_n$ which fix ∂D_n pointwise [10, Theorem 3].*

The set of isotopy classes of homeomorphisms $D_n \to D_n$ fixing $\partial D = \partial D_n$ pointwise is actually a group under composition, and is called the *mapping class group* of the pair (D, H_n) [1, Section 1.6], but for simplicity we will refer to it as the *mapping class group of D_n* since we will not be talking about other mapping class groups. Isotopy is like homotopy but for homeomorphisms, in that two maps are isotopic if they can be continuously deformed into one another. More exactly, we define it as

Definition 3.4. *Two self-homeomorphisms f_0, f_1 of a space X are* isotopic *if they can be included in a family $\{ f_t \}_{t \in I}$ of self-homeomorphisms of X such that the map $X \times I \to X$ taking (x, t) to $f_t(x)$ is continuous. Such a family is called an* isotopy*.*

3.2 The Burau Representation

The Burau representation is a representation introduced by Werner Burau in 1936. It is a (linear) representation of the braid group B_n by $n \times n$ matrices over the ring

$$\Lambda = \mathbb{Z}[t, t^{-1}].$$

This representation will be introduced along [1, Sections 3.1-3.3] and [10, Chapter 3].

We define the matrices corresponding to the Burau representation as follows: for $n \geq 2$, define the following matrices in $\mathrm{GL}_n(\Lambda)$, the group of invertible $n \times n$ matrices over Λ:

$$U_i = \begin{pmatrix} I_{i-1} & 0 & 0 & 0 \\ 0 & 1-t & t & 0 \\ 0 & 1 & 0 & 0 \\ 0 & 0 & 0 & I_{n-i-1} \end{pmatrix} \tag{3.6}$$

for $i = 1, 2, \ldots, n-1$. Here, I_k is the $k \times k$ identity matrix. When $i = i$ there is no unit matrix in the top left corner, and when $i = n-1$, there is no unit matrix in the bottom right corner.

Because of the way this matrix is structured, we can generally limit ourselves to blocks of these matrices. The most interesting block is the block

$$U = \begin{pmatrix} 1-t & t \\ 1 & 0 \end{pmatrix}.$$

One can verify by straightforward computation that

$$U^{-1} = \begin{pmatrix} 0 & 1 \\ t^{-1} & 1-t^{-1} \end{pmatrix} \in \mathrm{GL}_2(\Lambda).$$

And in this way, we can see that the U_i are invertible, with inverse

$$U_i^{-1} = \begin{pmatrix} I_{i-1} & 0 & 0 & 0 \\ 0 & 0 & 1 & 0 \\ 0 & t^{-1} & 1-t^{-1} & 0 \\ 0 & 0 & 0 & I_{n-i-1} \end{pmatrix}.$$

A prettier way of deriving this is by using the *Cayley-Hamilton theorem*, which states that any 2×2 matrix M over the ring Λ satisfies $M^2 - \mathrm{tr}(M)M + \det(M)I_2 = 0$, which for U means that $U^2 - (1-t)U - tI_2 = 0$. Since the unit matrices also satisfy this equation, we must have

$$U_i^2 - (1-t)U_i - tI_n = 0$$

which one can rewrite to find that [1]

$$U_i^{-1} = t^{-1}(U_i - (1-t)I_n).$$

This gives us precisely the inverse we gave above.

Because of the structure of U_i, it is obvious that $U_iU_j = U_jU_i$ for all i, j with $|i-j| \geq 2$. To verify the second braid relation (B2), we verify

$$\begin{pmatrix} 1-t & t & 0 \\ 1 & 0 & 0 \\ 0 & 0 & 1 \end{pmatrix} \begin{pmatrix} 1 & 0 & 0 \\ 0 & 1-t & t \\ 0 & 1 & 0 \end{pmatrix} \begin{pmatrix} 1-t & t & 0 \\ 1 & 0 & 0 \\ 0 & 0 & 1 \end{pmatrix} = \begin{pmatrix} 1 & 0 & 0 \\ 0 & 1-t & t \\ 0 & 1 & 0 \end{pmatrix} \begin{pmatrix} 1-t & t & 0 \\ 1 & 0 & 0 \\ 0 & 0 & 1 \end{pmatrix} \begin{pmatrix} 1 & 0 & 0 \\ 0 & 1-t & t \\ 0 & 1 & 0 \end{pmatrix}. \quad (3.7)$$

With this, Lemma 1.2 tells us that

$$\psi_n : B_n \to \mathrm{GL}_n(\Lambda) : \sigma_i \mapsto U_i \quad (3.8)$$

defines a group homomorphism for $n \geq 2$. We define ψ_1 to be the trivial homomorphism $B_1 \to \mathrm{GL}_n(\Lambda)$.

3.2.1 The Matrices

These matrices are very nice to work with, but it may be more interesting to see how they were come up with. Since the formal derivation for this requires some more topological knowledge, and is out of scope for this thesis, we will look at it mostly as a geometric idea, so this is by no means meant as a strict proof. The idea comes from [10, Chapter 3], where Jackson presents diagrams for the *reduced Burau representation*. We will use the approach he suggests to find the representation for

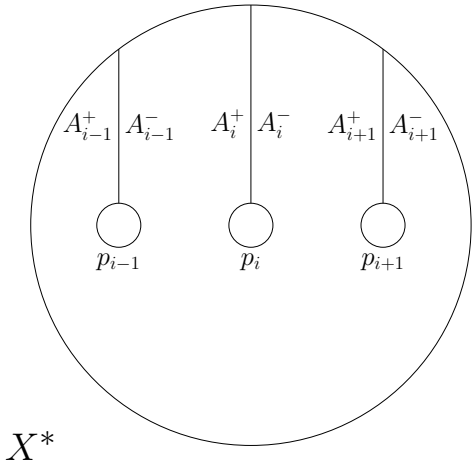

(a) The space X^*, obtained from the punctured disk D_{n+1} by enlarging the punctures, and cutting arcs down from them, creating two copies of those arcs A_i^+ and A_i^-.

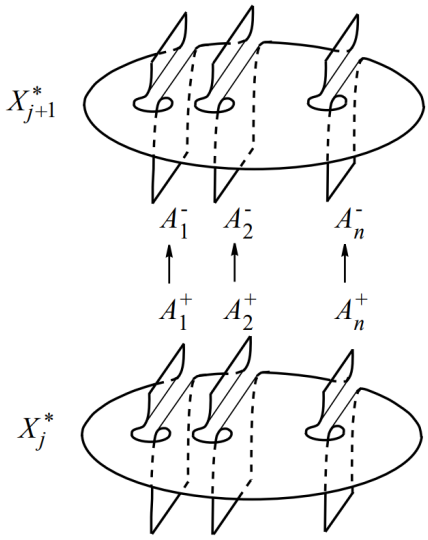

(b) Glueing the spaces X_j^*, image from [10, Figure 3.1].

Figure 3.4: Geometric construction of the space $\widetilde{X}$, a regular covering space of D_{n+1}.

the unreduced Burau representation that we discussed in the previous section. It uses the punctured disk, and the Dehn half-twists we saw in Section 3.1.

First of all, define the map

$$\phi : \pi_1(D_{n+1}) \to \mathbb{Z} \tag{3.9}$$

mapping a loop to its *total winding number*. In other words, for a loop

$$\alpha = \prod_{k=1}^{m} x_{i_k}^{\epsilon_k}$$

the total winding number is

$$\phi(\alpha) = \sum_{k=1}^{m} \epsilon_k.$$

We take $\widetilde{D}_{n+1}$ to be the *regular* covering space corresponding to the kernel of ϕ. A regular covering space is a covering space $\widetilde{X}$ of a space X (with covering map p) such that for every $x \in X$ and two points $\tilde{x}_1, \tilde{x}_2 \in p^{-1}(x)$, there exists a covering transformation $f \in \mathrm{Aut}(\widetilde{X})$ that maps $\tilde{x}_1$ to $\tilde{x}_2$. With *corresponding to* $\ker(\phi)$, it is meant that $\pi_1(\widetilde{X}) \cong \ker(\phi)$. We will not go into the details too much, but for example [7, Proposition 1.36] allows us to define $\widetilde{D}_{n+1}$ in this way.

We can find a geometric representation of $\widetilde{D}_{n+1}$ that will help us visualize. The first step for this is to enlarge the punctures to small disks. In the end, this will not change anything about the homotopy of our space. Then we cut down from these holes to the boundary of our disks, to create arcs A_i^+ and A_i^- (on either side of the cut) for each puncture p_i. Call this space X^*, see Figure 3.4a.

Define the obvious homeomorphisms $h_i : A_i^+ \to A_i^-$, taking each point in A_i^+ to the corresponding point in A_i^-. We can take countably many copies of the space X^*, which we label X_j^* for $j \in \mathbb{Z}$. Define the homeomorphisms $g_j : X_j^* \to X^*$ mapping a point $x \in X_j^*$ to its corresponding point in X^*. With these homeomorphism we can define a "glueing" map to define the space $\widetilde{X}$ by identifying the $A_i^+ \subset X_j^*$ with $A_i^- \subset X_{j+1}^*$ via $g_{j+1}^{-1} h_i g_j$, essentially glueing $A_i^+ \subset X_j^*$ to $A_i^- \subset X_{j+1}^*$. See Figure 3.4b.

On this space, we can define an action of $\mathbb{Z} = \langle t \rangle$, generated by

$$t : X_j^* \to X_{j+1}^* : x \mapsto g_{j+1}^{-1} g_j x.$$

The action t essentially shifts a point $x \in \widetilde{X}$ one level up.

We can convince ourselves that the fundamental group $\pi_1(\widetilde{X})$ of this space is indeed $\ker(\phi)$ as follows: We follow a loop in D_{n+1}, lifted to $\widetilde{X}$. Any time we encircle a puncture p_i of D_{n+1} clockwise (like the generator x_i), we cross $A_i^+ \subset X_j^*$ for whichever j we were in, and we go one level up. If we encircle it counterclockwise (like x_i^{-1}), we cross $A_i^- \subset X_j^*$, and we go down one level. In order for our lifted loop to end a the same point it started (so for it to actually be a loop), the total winding number has to be zero.

Using t, together with Dehn half twists, we can express the braid group as an action on the *first homology group* $H_1(\widetilde{X})$ of $\widetilde{X}$. The first homology group of a space is related to the first homotopy group. In fact, it can be seen as the group of *cycles*, essentially loops without a base point, or the abelianization of the fundamental group [7, Chapter 2]. It turns out that the group $H_1(\widetilde{X})$ is a $\mathbb{Z}[t, t^{-1}]$-*module* with a basis consisting of lifts of the n loops

$$u_i := x_i x_{n+1}^{-1}$$

for $i = 1, \ldots, n$. Here x_i is the loop around the ith puncture, as before. A module of a group over a ring is defined as follows.

Definition 3.5. *Let V be a vector space over a ring R and let G be a group. Then V is a module of G over R if a multiplication gv is defined for $g \in G$ and $v \in V$, satisfying the following conditions for all $u, v \in V$, $\lambda \in R$ and $g, h \in G$ [11, Definition 4.2]:*

(i) $gv \in V$;
(ii) $g(hv) = (gh)v$;
(iii) $1v = v$;
(iv) $g(\lambda v) = \lambda(gv)$;
(v) $g(u + v) = gu + gv$.

Modules are a very useful tool in finding (linear) representations of groups. If a group can be represented with matrices in a ring via $\rho : G \to \mathrm{GL}(n, R)$, this action of g on vectors v can be replaced by a matrix multiplication with the respective matrix $\rho(g)$ [11, Theorem 4.4]. The referenced theorem in fact states that every module corresponds to a representation, and every representation corresponds to a module. The matrices we find for the Burau representation are the matrices corresponding to the group action of B_n on the module $H_1(\widetilde{X})$ we mentioned.

The action of Dehn twists on the lifts of loops $x_i x_{n+1}^{-1}$ is shown in Figure 3.5. On the left hand side is the path, projected down onto the space X^*, on the right side is a diagram showing the level the path is in over time, along with the puncture that changes the level.

With these diagrams, the following relations can be derived:

$$\tau_i u_j = \begin{cases} u_i + t u_{i+1} - t u_i & \text{if } j = i \\ u_i & \text{if } j = i + 1 \\ u_j & \text{otherwise} \end{cases} \tag{3.10}$$

where tu_{i+1} indicates that the loop u_{i+1} happens "one level up", under the action of t. To be further convinced, one can draw more diagrams to see the intermediate steps,

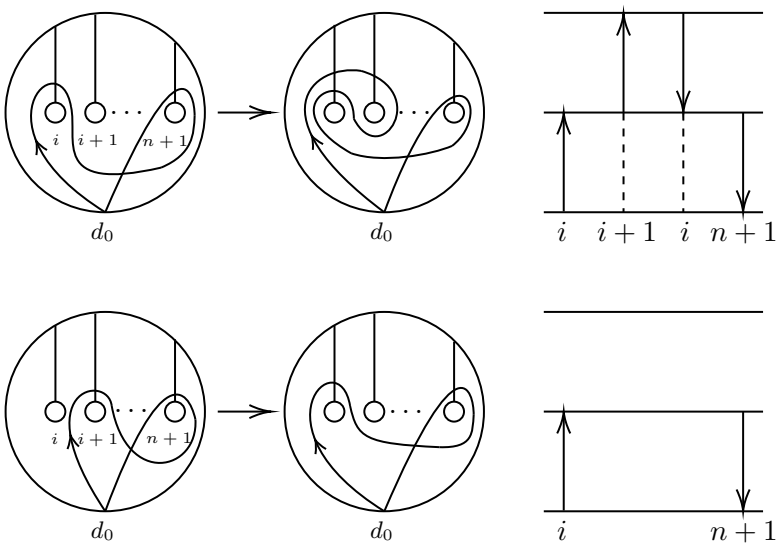

Figure 3.5: Diagrams showing the action of Dehn half-twists on the homology group of the space $\widetilde{X}$. The left hand side shows the space $\widetilde{X}$ projected down onto X^*, the right hand side shows the level of the path over time, along with the punctures it changes level at. The top figures show the action of τ_i on u_i, the bottom figures show the action of τ_i on u_{i+1}.

see Figure 3.6, keeping in mind that we are talking about homology, not homotopy and that the base point is there only for clarity. These relations give rise to the matrices U_i, relative to the basis $\{ u_1, \ldots, u_n \}$, recalling (3.6):

$$U_i = \begin{pmatrix} I_{i-1} & 0 & 0 & 0 \\ 0 & 1-t & t & 0 \\ 0 & 1 & 0 & 0 \\ 0 & 0 & 0 & I_{n-i-1} \end{pmatrix}$$

with multiplications with row vectors from the left. Transposing this matrix gives the same results, but multiplication would be from the right.

3.2.2 The Reduced Burau Representation

The representation we gave above turns out to be *reducible*.

Definition 3.6. *A linear representation $\rho : G \mapsto \mathrm{GL}(n, R)$ of a group G with a ring R is reducible if and only if it is equivalent to a representation ρ' (i.e. there is a matrix T such that $\rho(g) = T^{-1}\rho'(g)T$ for all $g \in G$) where all matrices are of the form [11, Equation (5.4)]*

$$\begin{pmatrix} X_g & 0 \\ Y_g & Z_g \end{pmatrix} \tag{3.11}$$

where X_g, Y_g and Z_g are matrices, and X_g is $k \times k$ for some $k \in \mathbb{Z}$.

Now, in representation theory it is nice to know about the irreducible representations of a group, since general representations are direct products of irreducible representations (as can be seen in the definition of reducibility). As mentioned before, Jackson gives a derivation of the matrices for the *reduced Burau representation* with the same arguments as the previous section [10], by looking at D_n instead of D_{n+1}, and using lifts of the loops $x_i x_{i+1}^{-1}$ as a basis for $H_1(\widetilde{D}_n)$.

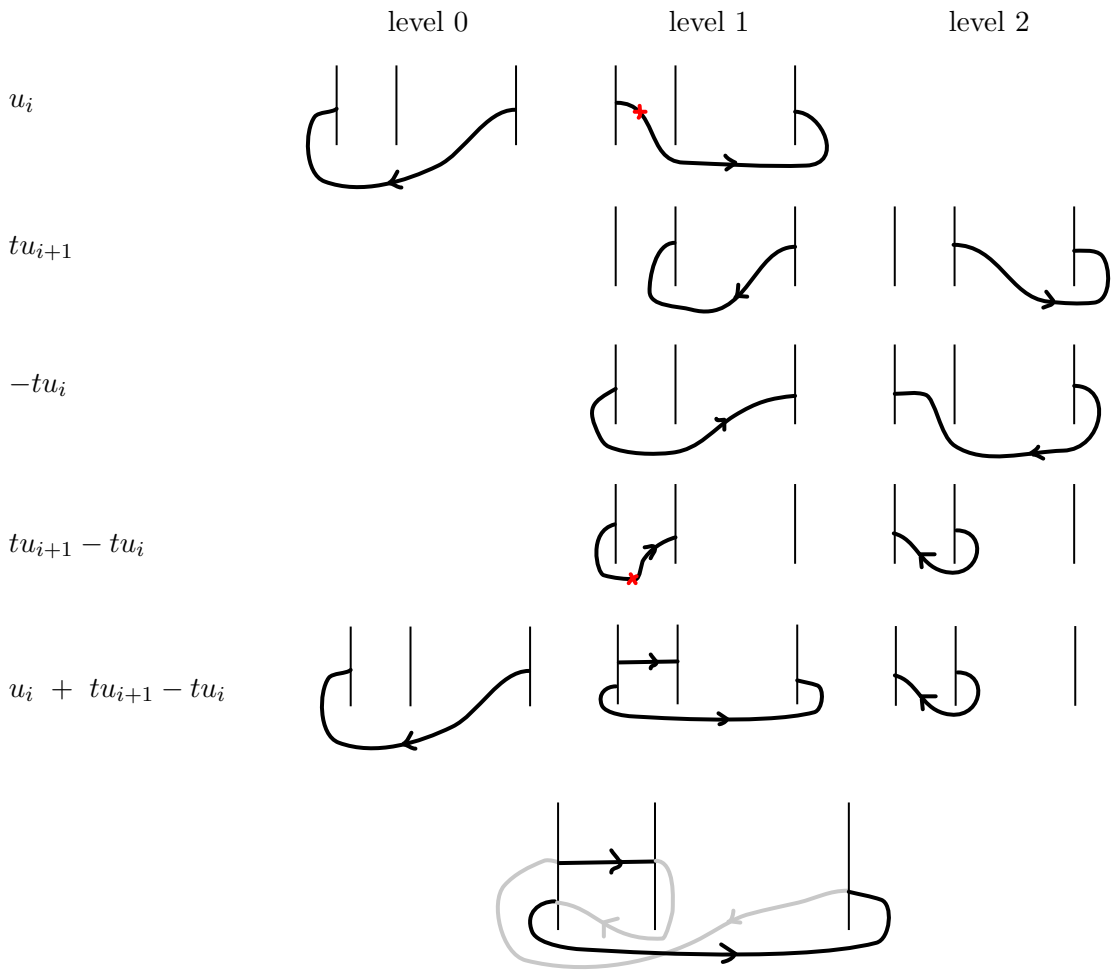

Figure 3.6: Diagram with intermediate steps to see that the right hand side of Figure 3.5 is indeed $u_i + tu_{i+1} - tu_i$. The vertical lines indicate the cuts corresponding to the punctures i, $i+1$ and n respectively. The other cuts have been left out. The holes have not been drawn explicitly, but are still at the bottom of the cuts. The red crosses indicate where the loop $tu_{i+1} - tu_i$ is "attached" (addition of loops) to u_i. The exact location of the cross does not matter. In fact, the loop $tu_{i+1} - tu_i$ can be "homotoped" down to level 0 or u_i up to level 2 to attach there.

Another way to derive the matrices for the reduced Burau representation is to consider a different basis $\{ u'_i \mid i = 1, \ldots, n \}$ for the first homology group of $\widetilde{X}$ from the previous section, with $u'_n = u_n$ and $u'_i = u_i - u_{i+1}$ otherwise, and deriving new relations for $\tau_i u'_j$. This way, one finds the matrices from Equation (3.12) [10].

Another, more abstract way of deriving them is by constructing the matrices corresponding to this reduced representation directly, as done in [1, Theorem 3.9]:

Lemma 3.7. *Let $n \geq 3$ and $V_1, V_2, \ldots, V_{n-1}$ be the $(n-1) \times (n-1)$ matrices over Λ given by*

$$V_1 = \begin{pmatrix} -t & 0 & 0 \\ 1 & 1 & 0 \\ 0 & 0 & I_{n-3} \end{pmatrix} \qquad V_{n-1} = \begin{pmatrix} I_{n-3} & 0 & 0 \\ 0 & 1 & t \\ 0 & 0 & -t \end{pmatrix}$$

and

$$V_i = \begin{pmatrix} I_{i-2} & 0 & 0 & 0 & 0 \\ 0 & 1 & t & 0 & 0 \\ 0 & 0 & -t & 0 & 0 \\ 0 & 0 & 1 & 1 & 0 \\ 0 & 0 & 0 & 0 & I_{n-i-2} \end{pmatrix}$$

for $i = 2, \ldots, n-2$. Then

$$C^{-1} U_i C = \begin{pmatrix} V_i & 0 \\ *_i & 1 \end{pmatrix} \tag{3.12}$$

where C is the $n \times n$ matrix

$$C = \begin{pmatrix} 1 & 1 & 1 & \cdots & 1 \\ 0 & 1 & 1 & \cdots & 1 \\ 0 & 0 & 1 & \cdots & 1 \\ \vdots & \vdots & \vdots & \ddots & \vdots \\ 0 & 0 & 0 & \cdots & 1 \end{pmatrix}$$

and $*_i$ is a row of length $n-1$ equal to 0 if $i < n-1$ and to $(0, \ldots, 0, 1)$ if $i = n-1$.

Proof. Call the matrix from Equation (3.12) V'_i. We need to show that $U_i C = C V'_i$. Note that the kth column of $U_i C$ is simply the sum of the first k columns of U_i. A direct computation shows that $U_i C$ is C with the (i,i)th entry set to $1 - t$ and the $(i+1, i)$th entry set to 1. Similarly, $C V'_i$ is obtained from C by the same modifications, noting that the kth row is the sum of the last $n - k$ rows of V'_i. □

Of course, the Braid relations can be verified for the matrices V_i directly, but we can also do it using the lemma we just proved. If the braid relations hold on the U_i, they must surely hold on the conjugates $C^{-1} U_i C$. The shape of this matrix from formula (3.12) implies that the matrices V_i then also satisfy the braid relations.

3.2.3 Faithfulness

An important property of a representation is its faithfulness. We take a quick look at the faithfulness of the unreduced Burau representation by considering the kernel of ψ_n, from (3.8). Obviously ψ_1 is faithful. The same can be verified quite easily for ψ_2 by considering $\psi_2(\sigma_1)$, which has an eigenvector $(-t, 1)$ with eigenvalue $-t$. Therefore, it cannot be of finite order. For $n = 3$ faithfulness can be shown via the reduced Burau representation [1, Section 3.3.2], but for $n = 4$ it is still an open problem [8, `Burau Representation`].

For $n \geq 5$, it has been shown that the Burau representation is *not* faithful. Note that $\ker \psi_n \subset \ker \psi_{n+1}$ under the inclusion $B_n \subset B_{n+1}$. So if $\ker \psi_n \neq \{ 1 \}$ then

$\ker \psi_m \neq \{ 1 \}$ for all $m \geq n$. Stephen Bigelow has shown that indeed $\ker \psi_5 \neq \{ 1 \}$, and even found an example of a non-trivial braid (of length 120 in the generators) in the kernel of ψ_5 [12].

3.3 The Lawrence-Krammer-Bigelow Representation

Another representation of the braid group B_n is one introduced by R. Lawrence and studied by D. Krammer and S. Bigelow. It arises from the configuration space of two particles on the punctured disk. Matrices have been derived for this representation, but it is significantly more complex than the Burau representation. In this section, I want to present the matrices and give a short idea of what the derivation of this presentation is like. I will present the matrices as given by [13] and the idea of the derivation of the presentation presented in [1].

The matrices for the representation of B_n are $m \times m$ matrices over the ring

$$R = \mathbb{Z}[q^{\pm 1}, t^{\pm 1}] \tag{3.13}$$

for two invertible elements q and t and $m = n(n-1)/2$. With respect to a basis

$$\{ x_{1,2}, x_{1,3}, x_{2,3}, x_{1,4}, x_{2,4}, \ldots, x_{n-1,n} \}$$

for a module V of R the matrices for the representation are given by the following relations [13]:

$$\sigma_k x_{i,j} = \begin{cases} x_{i,j} & k \notin \{ i-1, i, j-1, j \} \\ qx_{k,j} + (q^2 - q)x_{k,i} + (1-q)x_{i,j} & k = i-1 \\ x_{i+1,j} & k = i \neq j-1 \\ qx_{i,k} + (1-q)x_{i,j} - (q^2-q)tx_{k,j} & k = j-1 \neq i \\ x_{i,j+1} & k = j \\ -tq^2 x_{i,j} & k = i = j-1 \end{cases} \tag{3.14}$$

Krammer himself gives other relations in [14] which result in even more complex matrices.

One can show that the matrices defined by these relations in fact satisfy the braid relations, and thus define a representation, but this is a very tedious task. I generated the matrix for $\sigma_3 \in B_4$ below, just to give some illustration that these matrices are not trivial to work with.

$$\sigma_3 \in B_4 \text{ corresponds to } \begin{pmatrix} 1 & 0 & 0 & 0 & 0 & 0 \\ 0 & 0 & 0 & q & 0 & 0 \\ 0 & 0 & 0 & 0 & q & 0 \\ 0 & 1 & 0 & 1-q & 0 & -tq^2 \\ 0 & 0 & 1 & 0 & 1-q & 0 \\ 0 & 0 & 0 & q^2-q & q^2-q & 0 \end{pmatrix}. \tag{3.15}$$

I will now sketch how one gets to this representation along [1, Section 3.5]. We start by considering $F_2(D_n)$ and $Q_2(D_n)$, the configuration spaces of 2 distinguishable and indistinguishable particles on the n-punctured disk D_n respectively. Denote a point in $Q_2(D_n)$ by $\{x, y\}$, corresponding to associated points $(x, y), (y, x) \in F_2(D_n)$. A path ξ in $Q_2(D_n)$ can be written as $\{\xi_1, \xi_2\}$ with ξ_1, ξ_2 paths in D_n. The path ξ is a loop if

$$\{\xi_1(0), \xi_2(0)\} = \{\xi_1(1), \xi_2(1)\}$$

so that either

$$(i)\ \xi_1(0) = \xi_1(1) \neq \xi_2(0) = \xi_2(1) \qquad \text{or} \qquad (ii)\ \xi_1(0) = \xi_2(1) \neq \xi_1(1) = \xi_2(0).$$

In case (i), the loops ξ_1 and ξ_2 are also loops in D_n. In case (ii) they are not, but the concatenation $\xi_1\xi_2$ of these loops is. We define two invariants u and w on loops in $Q_2(D_n)$. Consider a loop $\xi = \{\xi_1, \xi_2\}$ in $Q_2(D_n)$. We define $w(\xi)$ to be:

$$w(\xi) = \begin{cases} w(\xi_1) + w(\xi_2) & \text{if } \xi \text{ is of case } (i) \\ w(\xi_1\xi_2) & \text{if } \xi \text{ is of case } (ii) \end{cases} \tag{3.16}$$

where $w(\xi_i)$ is the total winding number of the loop ξ_i around the punctures in D_n, like the map ϕ from Equation (3.9). We define u using the map

$$I \to S^1 : s \mapsto \frac{\xi_1(s) - \xi_2(s)}{|\xi_1(s) - \xi_2(s)|}$$

which sends $s = 0$ and $s = 1$ to either opposite points (in case (ii)) or equal points (in case (i)). The map

$$I \to S^1 : s \mapsto \left(\frac{\xi_1(s) - \xi_2(s)}{|\xi_1(s) - \xi_2(s)|} \right)^2 \tag{3.17}$$

is then a loop on S^1. Recall that the fundamental group of S^1 is the infinite cyclic group generated by the single loop around S^1, as seen in Example 2.12. We can associate the loop (3.17) with k times this generator for some $k \in \mathbb{Z}$, and set $u(\xi) = k$. Note that u is odd if and only if the loop is of case (ii). The invariant u can be seen as the winding number of the two loops ξ_1 and ξ_2 "around each other". Also note that u and w are preserved under homotopy, and additive under multiplication of loops.

We consider two important examples. The first of which is a loop $\xi = \{\xi_1, \xi_2\}$ where ξ_1 is the constant loop, and ξ_2 is a loop winding around a single puncture once, but not around ξ_1. Then $u(\xi) = 0$ and $w(\xi) = w(\xi_1) + w(\xi_2) = 1$.

For another example, choose a counterclockwise, non-constant loop in D_n, not encircling any punctures. Split this loop into two parts ξ_1 and ξ_2. Then for the loop $\xi = \{\xi_1, \xi_2\}$, we have $u(\xi) = 1$ and $w(\xi) = w(\xi_1\xi_2) = 0$.

With these invariants, we can construct a group homomorphism, taking $c = \{d_1, d_2\}$ to be a base point with d_1, d_2 distinct points in the boundary of the unit disk ∂D. This homomorphism is defined as

$$\varphi : \pi_1(Q_2(D_n), c) \to \mathbb{Z} \times \mathbb{Z} : \quad \xi \mapsto q^{w(\xi)} t^{u(\xi)}.$$

Here, we represent $\mathbb{Z} \times \mathbb{Z}$ as $\langle q \rangle \times \langle t \rangle$. The map φ is a homomorphism because of the invariance under homotopy and additiveness under multiplication of loops of u and w. This homomorphism is also surjective because the examples we discussed in fact map to the generators of $\mathbb{Z} \times \mathbb{Z}$.

Using this, we can construct a covering space $\widetilde{\mathcal{Q}}$ of $Q_2(D_n)$, corresponding to the kernel of φ. This makes it so that

$$\mathrm{deck}(\widetilde{\mathcal{Q}}) \simeq \varphi(\pi_1(Q_2(D_n))) = \mathbb{Z} \times \mathbb{Z}, \tag{3.18}$$

see [7, Proposition 1.39]. The induced action of q and t on the homology of this space (more specifically, on the "relative homology group" $H_2(\widetilde{\mathcal{Q}}, \mathbb{Z})$), turns this group into a module over the commutative ring

$$R = \mathbb{Z}[q^{\pm 1}, t^{\pm 1}],$$

the "group ring" of $\mathbb{Z} \times \mathbb{Z}$ over $\mathbb{Z}$. The braid group representation will follow from the action of the braid group B_n on this homology group. We associate B_n with the mapping class group of D_n, as we saw in Section 3.1. We can take a self-homeomorphism f of D_n from this group, which then induces a homeomorphism $\widehat{f} : Q_2(D_n) \to Q_2(D_n)$ via

$$\widehat{f}(\{x, y\}) = \{f(x), f(y)\}$$

where x, y are distinct points in D_n. Clearly, since f fixes the boundary ∂D of the unit disk, we have $\widehat{f}(c) = c$. This means $\widehat{f}$ induces an automorphism $\widehat{f}_\#$ of $\pi_1(Q_2(D_n), c)$. An important property of this homomorphism is that it preserves the invariant φ:

Lemma 3.8. *The induced homomorphism $\widehat{f}_\#$ preserves the invariant φ. In other words, we have $\varphi \circ \widehat{f}_\# = \varphi$.*

Proof. For the equality, it is needed that $w \circ \widehat{f}_\# = w$ and $u \circ \widehat{f}_\# = u$. The first equality follows from the fact that f preserves the total winding number for small loops encricling only one of the punctures of D_n, and arbitrary loops are products of these loops. The argument for small loops is that one only has to consider the encircled puncture. After all, the image of the enclosed area has to be homeomorphic to the enclosed area, which is homeomorphic to D_1. To verify that orientation is also preserved, note that the small loop can be homotoped to the boundary of the disk. The image under the homeomorphism f results in the same loop, in the same orientation, and thus the same winding number. The induced maps $\widehat{f}$ and $\widehat{f}_\#$ must then also preserve this quantity.

For the second equality, consider the inclusion $Q_2(D_n) \to Q_2(D)$ induced by the inclusion $D_n \to D$. We can define the invariant u on $Q_2(D)$ in the exact same way we did for D_n, and find an invariant of loops in D. The *Alexander-Tietze theorem* states that any self-homeomorphism on D is isotopic to identity, so the self-homeomorphism of $Q_2(D)$ induced by f must be homotopic to identity as well. Then $u \circ \widehat{f}_\# = u$ on D, and so it is on D_n as well. Thus, we conclude that $\phi \circ \widehat{f}_\# = \phi$. □

Since $\widehat{f}_\#$ preserves φ, the map $\widehat{f}$ that induced it lifts uniquely to a map $\widetilde{f} : \widetilde{\mathcal{Q}} \to \widetilde{\mathcal{Q}}$. This follows from the *lifting criterion* ([7, Proposition 1.33] for example). It also implies that $\widetilde{f}$ commutes with the deck transformations of $\widetilde{\mathcal{Q}}$.

All of this makes it so B_n can be mapped to a transformations on the earlier mentioned homology group of $Q_2(D_n)$, induced by $\widetilde{f}$. For the derivation of the matrices, the adept mathematician can refer to [13].

3.3.1 Some properties

The Lawrence-Krammer-Bigelow representation has some important properties that are worth mentioning. The first property is that this representation is faithful for all $n \geq 1$. This can be shown by looking at the matrices, done by Krammer in [14], or it can be done topologically, as in [1, Sections 3.6-3.7].

The second property is that this representation makes the braid groups *linear*. This is Theorem 3.16 in [1].

Definition 3.9. *A group G is called linear if there is an injective group homomorphism $G \to \mathrm{GL}_n(\mathbb{R})$ for some integer $n \geq 1$.*

This follows from the matrix representation over the ring $\mathbb{Z}[q^{\pm 1}, t^{\pm 1}]$ by embedding it in the real numbers by assigning two *algebraically independent* real numbers to q and t. Algebraically independent here means there is no non-trivial polynomial with coefficients in $\mathbb{Z}$ that solves for q and t. Replacing q and t by these numbers in the matrices given by the representation gives us the homomorphism we are looking for.

Chapter 4

Anyons

In this chapter, we will explore an application of braid groups in physics. In Chapter 2, we discussed configurations of distinguishable and indistinguishable particles on manifolds. In quantum physics, the distinguishablility of particles in a system plays an important role in the properties of the system. It might feel natural to impose certain symmetries on a system under the *exchange* of two particles.

An example of this might be the following (see [15, Chapter 13]). Suppose we have a system of two indistinguishable particles in 3D space in a state $|a, b\rangle$. The physical meaning of the states a and b does not matter much, but they may for example be eigenstates of some operator like momentum or spin. Note that the order of the states a, b itself has no significance, after all the particles are indistinguishable, so how would we know which is in state a, and which is in state b? The state $|b, a\rangle$ must be physically identical to the state $|a, b\rangle$ though, so we require that these states only differ by a phase:

$$\begin{aligned} |a, b\rangle &= e^{i\theta_{ab}} |b, a\rangle \\ |b, a\rangle &= e^{i\theta_{ba}} |a, b\rangle \end{aligned} \tag{4.1}$$

where θ_{ab} and θ_{ba} may depend on a and b. This implies that

$$e^{i\theta_{ab}} e^{i\theta_{ba}} = 1. \tag{4.2}$$

With this, we can define the states

$$\begin{aligned} |a, b\rangle' &= e^{-i\theta_{ab}/2} |a, b\rangle \\ |b, a\rangle' &= e^{-i\theta_{ba}/2} |b, a\rangle \end{aligned}$$

such that

$$|b, a\rangle' = e^{-i\theta_{ba}/2} |b, a\rangle = e^{i\theta_{ba}/2} |a, b\rangle = e^{i(\theta_{ab}+\theta_{ba})/2} |a, b\rangle' = \pm |a, b\rangle' .$$

This derivation works in three spatial dimensions (or more), but it does not work in 2D space! This is mostly because exchanging particles in two spatial dimensions is not necessarily as simple as equation (4.2) makes it out to be. In this chapter, we will discuss why that is. A consequence of this is that the statistics of particles in 2D is not necessarily that of fermions or bosons, like it is in three or more dimensions. We will consider different configuration spaces, and see what statistics these particles do follow. Then we will study an abstract construction of these particles by Leinaas and Myrheim [4], alongside physical constructions by Frank Wilczek [2]. In the last section, we will look at where anyons play a role in the Fractional Quantum Hall Effect.

4.1 Exchanging Particles

As mentioned before, when looking at systems of indistinguishable particles, an exchange of particles results in a system that is physically identical, such that for example the wave function only differs by a phase. The wave function might also differ by a matrix or some other operator, but in this chapter we will only be looking at "abelian anyons", so we assume it is a phase. What this phase is, depends on the braid group on N strands on a manifold M. More specifically, it depends on unitary, one-dimensional representations of it. The wave function of the system has to obey the structure of this group. One can also observe multi-dimensional representations, in the case of "non-abelian anyons" [9, Chapter 3].

In Chapter 2 we have already seen some examples of configuration spaces of specific manifolds. In this section, we are going to elaborate a bit on these examples. We can find unitary, one-dimensional representations of their braid groups, which in these examples are connected to the statistics of the system. We do this along [9, Chapter 3].

First, to introduce a small bit of notation, we denote the *abelianization* of a group G by

$$[G]_{ab} := G/[G,G], \tag{4.3}$$

where $[G,G]$ denotes the commutator subgroup of G.

Since one-dimensional representations of groups are abelian, we must abelianize the braid group of the system we are considering. As an illustration, we can abelianize the Artin braid group in a few steps.

Lemma 4.1. *The braid groups B_n for $n \geq 1$ are generated by the two elements σ_1 and $\alpha := \sigma_1\sigma_2\dots\sigma_{n-1}$ [1, Exercise 1.1.4].*

Proof. We can prove this by induction. First, we prove the relation

$$\sigma_i^{-1}\sigma_{i+1}\sigma_i = \sigma_i^{-1}\sigma_{i+1}\sigma_i\sigma_{i+1}\sigma_{i+1}^{-1} = \sigma_i^{-1}\sigma_i\sigma_{i+1}\sigma_i\sigma_{i+1}^{-1} = \sigma_{i+1}\sigma_i\sigma_{i+1}^{-1} \tag{$*$}$$

for $i = 1,\dots,n-2$. Suppose σ_i can be written as a word in σ_1 and α. Then

$$\begin{aligned}
\alpha\sigma_i\alpha^{-1} &= \sigma_1\sigma_2\dots\sigma_{n-1}\sigma_i\sigma_{n-1}^{-1}\dots\sigma_2^{-1}\sigma_1^{-1} \\
\text{(using (B1))} \quad &= \sigma_1\sigma_2\dots\sigma_i\sigma_{i+1}\sigma_i\sigma_{i+1}^{-1}\sigma_i^{-1}\dots\sigma_2^{-1}\sigma_1^{-1} \\
\text{(using (*))} \quad &= \sigma_1\sigma_2\dots\sigma_i\sigma_i^{-1}\sigma_{i+1}\sigma_i\sigma_i^{-1}\dots\sigma_2^{-1}\sigma_1^{-1} \\
&= \sigma_1\sigma_2\dots\sigma_{i-1}\sigma_{i+1}\sigma_{i-1}^{-1}\dots\sigma_2^{-1}\sigma_1^{-1} \\
\text{(using (B1))} \quad &= \sigma_{i+1}.
\end{aligned}$$

And so, by induction, this proves the lemma. □

More importantly, this proof also proves that all generators σ_i are conjugate. This implies that all generators map to the same element in $[B_n]_{ab} = B_n/[B_n,B_n]$. After all, for two generators σ_i, σ_j, where $\sigma_i = \beta\sigma_j\beta^{-1}$ for some $\beta \in B_n$ we have

$$\sigma_i[B_n,B_n] = \sigma_i\beta\sigma_j^{-1}\beta^{-1}\sigma_j[B_n,B_n] = \sigma_i\sigma_i^{-1}\sigma_j[B_n,B_n] = \sigma_j[B_n,B_n],$$

since $\beta\sigma_j^{-1}\beta^{-1}\sigma_j$ is a commutator. So $[B_n]_{ab}$ is cyclic and generated by a single generator (the image of any of the generators). We can call this generator σ^{ab}. The abelianized braid group is also infinite, since we can map any generator to $1 \in \mathbb{Z}$ and find a surjective homomorphism. For example, the word σ_1^k maps to k. Thus, $[B_n]_{ab}$ is an infinite cyclic group with generator σ^{ab}.

The scalar quantum statistics will be numbered by the homomorphism group

$$\hom\left([\pi_1(Q_N(M))]_{ab}, \mathcal{U}(1)\right), \tag{4.4}$$

where $\mathcal{U}(1)$ is the one dimensional unitary group [9].

4.1.1 In The Plane

We have seen that the fundamental group of the configuration space for N indistinguishable particles in the plane is B_N, and that of distinguishable particles is the pure braid group P_N. We just deduced that $[B_N]_{ab} \cong \mathbb{Z}$. We have

$$\hom(\mathbb{Z}, \mathcal{U}(1)) = \mathcal{U}(1),$$

since any homomorphism of $\mathbb{Z}$ is defined by where it maps 1, which can be any value in $\mathcal{U}(1)$. Similarly, every element in $\mathcal{U}(1)$ defines a homomorphism in this way. We could also have defined the image of the generators directly as $e^{i\theta}$ for some $\theta \in (-\pi, \pi]$. We can take any value for θ in this range, since there are no further restrictions imposed on σ_i, and thus on θ. Note that $\theta = 0$ corresponds to boson statistics, and $\theta = \pi$ to fermion statistics. Any value inbetween corresponds to *fractional statistics*, or anyons! One thing to mention though, is that the term *fractional statistics* is not entirely accurate, since depending on the setup, it is not necessarily restricted to only fractional values.

4.1.2 In $\mathbb{R}^3$

Another example we saw in Chapter 2 was the configuration space of particles in $\mathbb{R}^3$. We found that (recalling (2.18))

$$\pi_1(Q_N(\mathbb{R}^3)) \cong S_N.$$

We know that S_N satisfies the same relations as B_N for the generators s_i, as well as the relation

$$s_i^2 = 1$$

for $i = 1, \ldots, n-1$. This means we can do the same sort of derivation as we did for the plane in Lemma 4.1 to conclude that the abelianization of the braid group on $Q_N(\mathbb{R}^3)$ is generated by one element s^{ab}. The extra relation above imposes the relation

$$(s^{ab})^2 = 1,$$

and we find that

$$[\pi_1(Q_N(\mathbb{R}^3))]_{ab} \cong \mathbb{Z}_2.$$

This implies that, unsurprisingly, we only have two choices for the phase caused by the exchange of particles: $\theta = 0$, for boson statistics, and $\theta = \pi$, for fermion statistics.

4.1.3 On the sphere S^2

We have not seen the configuration space for the sphere in Chapter 2, so we will look at it briefly. It is physically less relevant, but the results are interesting.

We can represent paths on the sphere in the same way we did for geometric braids, see Figure 4.1. In this diagram, the braid $\sigma_1\sigma_2\sigma_3^2\sigma_2\sigma_1$ is shown. Note that we can slip the strand labeled 1 around the sphere to turn this into the trivial braid. This can be generalized into an additional relation on the generators of the braid group on S^2:

$$\sigma_1\sigma_2 \ldots \sigma_{N-2}\sigma_{N-1}^2\sigma_{N-2} \ldots \sigma_2\sigma_1 = 1. \tag{4.5}$$

Using the same reasoning as before, this imposes an additional relation on the generator σ^{ab} of the abelianized braid group, namely

$$(\sigma^{ab})^{2N-2} = 1,$$

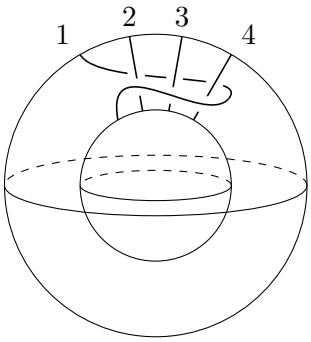

Figure 4.1: An example of a braid on a sphere. It can be noted that the strand labeled 1 may be slipped around the sphere to turn this into the trivial braid [9, Figure 2.8].

implying that

$$\pi_1(Q_N(S^2)) \cong \mathbb{Z}_{2N-2}.$$

This restricts our choice of the value for θ to the values

$$\theta = \frac{k\pi}{N-1} \tag{4.6}$$

with $k = 0, 1, \ldots, 2N-3$. Fermion statistics arise in the case where $k = N-1$, and boson statistics for $k = 0$.

4.2 The Anyon Phase

We have now seen that anyons can exist in certain setups, with a certain parameter θ. This parameter is dependent on the dynamics of the system. Its value will turn out to be characteristic for the system that is observed. In this section, we will to take a closer look at this parameter, along a very rigorous derivation by Leinaas and Myrheim in [4]. Alongside this, we study a physical construction, which is essentially an application of this general theory, given by Frank Wilczek [2] in the article where he first coins the term *anyons*.

4.2.1 Some Differential Geometry

To understand the generic construction a bit better, we will first need a bit of differential geometry. This is where the theory of gauges and gauge transformations finds its roots. I will introduce this along [16, Chapter 7]. Most importantly, we want to take a look at *parallel transport*. Before we look at that, we must introduce some other concepts. First of which is the notion of a *fiber bundle*. This concept is closely related to covering spaces, which had discrete fibers. The main difference is that now fibers are general spaces (and can even be vector spaces).

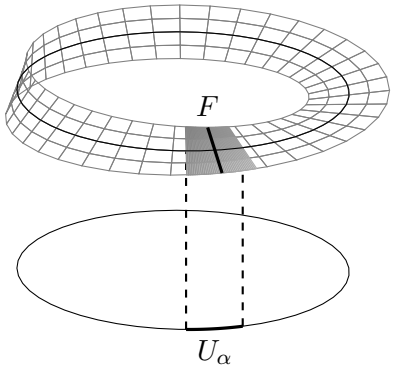

Figure 4.2: The Möbius band as an example of a fiber bundle.

Definition 4.2. *A fiber bundle $(\widetilde{X}, p, F, G, X)$ is a collection of the following objects:*

(i) A topological space $\widetilde{X}$, called the total space.

(ii) A topological space X called the base space, *and a projection $p : \widetilde{X} \to X$ of $\widetilde{X}$ onto X.*

(iii) A topological space F called the fiber.

(iv) A group G of homeomorphisms of the fiber F, called the structure group.

(v) A set of open neighborhoods U_α covering X which reflect the "triviality" of $\widetilde{X}$. More specifically, for each U_α, there is a homeomorphism

$$\phi_\alpha : p^{-1}(U_\alpha) \to U_\alpha \times F$$

where ϕ_α satisfies

$$p \circ \phi^{-1}(x, f) = x \quad \textit{with} \quad x \in U_\alpha, f \in F.$$

Definition 4.3. *A* principal bundle *is a fiber bundle with its structure group as its fiber. In this case the transition functions ϕ act on the fiber by left translations.*

Essentially what fiber bundles allow us to do, is to observe local properties of a space as if they were products, even though globally, the space might not be a product. A nice example of a fiber bundle is the Möbius strip. Globally, the Möbius strip is not a product. It looks like the cylinder with a twist. The cylinder is a product $S^1 \times I$ of the circle and an interval (for example the unit interval $I = [0, 1]$). It turns out that locally, we *can* view the Möbius strip as a cylinder. The Möbius strip is the total space of a fiber bundle with the circle S^1 as base space, a line segment as fiber, but what is the structure group? The structure group arises from the transitions between the open sets U_α covering the base space. These open sets may overlap, so we can check what happens in this overlapping region. Consider two open neighborhoods U_α, U_β in the covering of X, with homeomorphisms ϕ_α, ϕ_β respectively. Then

$$\phi_\alpha \circ \phi_\beta^{-1} : (U_\alpha \cap U_\beta) \times F \to (U_\alpha \cap U_\beta) \times F$$

is a continuous, invertible map. If we fix $x \in U_\alpha \cap U_\beta$, and vary f, then $\phi_\alpha \circ \phi_\beta^{-1}$ is a map from F to F. We can label this map $g_{\alpha\beta}$, and call it a *transition map*. The set of these maps $F \to F$ form the structure group G. In the case of the Möbius strip, maps $g_{\alpha\beta}$ must map the interval I to itself homeomorphically, which can only be done by either the identity, or by "flipping the interval", and we find that the structure group for the Möbius strip is the group $\mathbb{Z}_2$. The Möbius strip can also be defined as a

principal bundle, if the fiber is replaced with $\mathbb{Z}_2$, essentially leaving us with the edge of the strip.

Another example of a bundle, one that gets us closer to the notion of parallel transport, is the *tangent bundle*, and is defined as

$$T(M) := \bigcup_{x \in M} T_x(M), \tag{4.7}$$

which has base space M and the tangent space $T_x(M)$ as fiber (essentially equivalent to $\mathbb{R}^n$ with $n = \dim M$) at point $x \in M$. Now it turns out that the structure group of this space is $\mathrm{GL}_n(\mathbb{R})$, and that the transition functions $g_{\alpha\beta}$ are the Jacobian matrices for the change of variables from the local coordinates at x_α to x_β. This can be derived by looking at the same tangent vector in two overlapping sets U_α, U_β with their respective local coordinate system in $T_{x_i}(M)$, $i = \alpha, \beta$, done in [16, Section 7.3].

We need some other important concepts before we describe what parallel transport is, namely that of a *vertical subspace* and a *horizontal subspace*. We start off with a principal bundle P with structure group (and simultaniously fiber) G over a manifold M. The *vertical subspace* $V_x(P) \subseteq T_x(P)$ is the subspace of the tangent space of P at a point $x \in P$, such that every vector is tangent to the fiber. This can easily be visualized in the example of the Möbius band. Along with the vertical subspace, there is a horizontal subspace $H_x(P) \subseteq T_x(P)$ such that

$$T_x(P) = V_x(P) \oplus H_x(P).$$

Here $\oplus$ denotes the direct sum. Note that this does not define $H_x(P)$ uniquely. If our bundle sits within a vector space, the horizontal space may for example be defined as the space orthogonal to $V_x(P)$. Generally, this definition is made unique by defining $H_x(P)$ along a *connection*. A formal definition of a connection can be found in [17, Chapter 16]. In chapter 9, Frankel [17] also defines an *affine connection*, or *covariant differentiation*, which is essentially a connection for *vector bundles*. Vector bundles are fiber bundles where the fiber is also a vector space. Since the concept of a covariant derivative is easier to explain than that of a general connection, and since it is really the only relevant case for us now, we will look at covariant derivatives instead. The formal definition is in [17, Section 9.1]. In order to not get side tracked too much, I will not provide the definition here, but the idea is that it is essentially a derivative that "transforms along with the manifold", and depends on the local neighborhood. It is a derivative that corrects for the change in local coordinates when moving around on a manifold.

This derivative can be looked at a bit more closely, we will need it for Leinaas and Myrheim's construction anyway. We consider the principal bundle P locally, with local coordinates (x, g) with $x \in M$, $g \in G$. The basis for the vertical subspace $V_x(P)$ are the vectors

$$\frac{\partial}{\partial g_i}, \quad \text{with } i = 1, 2, \ldots, \dim G.$$

Here we use a convention where we view basis vectors as directional derivatives. For example for a curve γ, its partial derivative to the coordinate g_i shows the coordinate of its tangent vector in the direction $\frac{\partial}{\partial g_i}$.

The basis for $H_x(P)$ can be given by

$$D_\mu = \frac{\partial}{\partial x_\mu} + \Gamma^\mu_{ij} g_j \frac{\partial}{\partial g_i} \tag{4.8}$$

for $\mu = 1, \ldots, \dim M$ [16, Section 7.10]. We use the Einstein summation principle here. The Γ^μ_{ij} are called the *Christoffel symbols*, and they depend on the manifold,

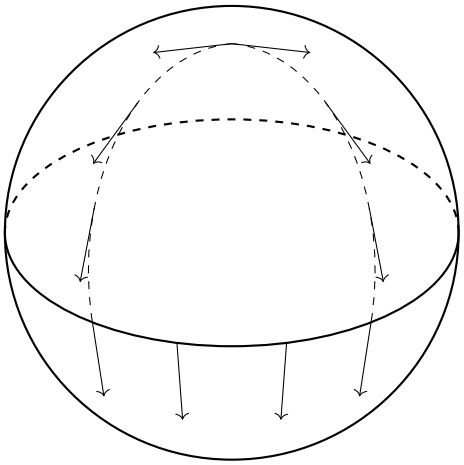

Figure 4.3: A classic example of a vector being parallel transported on a sphere.

and the position in the bundle P. The operator D_μ is known as a *covariant derivative*. The Christoffel symbols are dependent on the connection, also known as the *gauge potential*. A more precise definition of these can be found in [16, Section 7.10, 7.15].

Now we can define parallel transport. Take a curve $\gamma : I \mapsto M$ and a point $x_0 \in P$. This curve γ can be *horizontally lifted* uniquely to a curve $\tilde{\gamma} : I \mapsto P$ with $\tilde{\gamma}(0) = x_0$, such that the tangent vector of $\tilde{\gamma}$ is always horizontal, or in other words: $\frac{\mathrm{d}}{\mathrm{d}t}\tilde{\gamma}(t) \in H_{\tilde{\gamma}(t)}(P)$ for all $t \in I$. Lifted here means that $p \circ \tilde{\gamma} = \gamma$, similar to lifting for covering spaces. With this, we can define the parallel transport of a fiber from a point x to a point x' in P. We do this by taking any $u \in p^{-1}(x)$ and constructing the unique horizontal lift $\tilde{\gamma}$ of γ starting at u. We map u to $\tilde{\gamma}(1) := u' \in p^{-1}(x')$, the ending point of $\tilde{\gamma}$.

This is a very abstract definition of parallel transport, but we can provide a simpler example. A classic example is a vector being transported on a sphere from the north pole, down to the equator, then moved 90 degrees around the equator and back up to the north pole. When keeping this vector parallel, it is rotated 90 degrees upon returning to the north pole, see Figure 4.3. A more relevant example is that of our two-anyon system in the plane, from Section 4.1.1. Recall Figure 2.7, and consider Figure 4.4. In Chapter 2 the relative space $r(2,2)$ was shown as the punctured plane, but this was not accurate. It is more accurately represented as a cone with a vertex angle of 30 degrees (this preserves the lengths of paths). With this, there is now curvature in the space, and a vector parallel transported around the vertex of the cone flips direction once.

Now to look a bit closer at the horizontal lift, note that the tangents of $\tilde{\gamma}(t) = (x(t), g(t))$ are given by

$$\frac{\mathrm{d}}{\mathrm{d}t} = \dot{x}_\mu \frac{\partial}{\partial x_\mu} + \dot{g}_j \frac{\partial}{\partial g_j}, \tag{4.9}$$

where we again associate vectors with differential operators and use Einstein's summation convention. Since we require that this lift is horizontal, we must have

$$\frac{\mathrm{d}}{\mathrm{d}t} = \dot{x}_\mu \frac{\partial}{\partial x_\mu} + \dot{g}_j \frac{\partial}{\partial g_j} = \beta^\mu \left(\frac{\partial}{\partial x_\mu} + \Gamma^\mu_{ij} g_i \frac{\partial}{\partial g_j} \right),$$

from which follows that $\beta^\mu = \dot{x}_\mu$. This equation also gives us the following first order linear differential equation:

$$\dot{g}(t) - b(x)g(t) = 0 \tag{4.10}$$

for a certain function $b(x)$. This equation is known as the *parallel transport equation*.

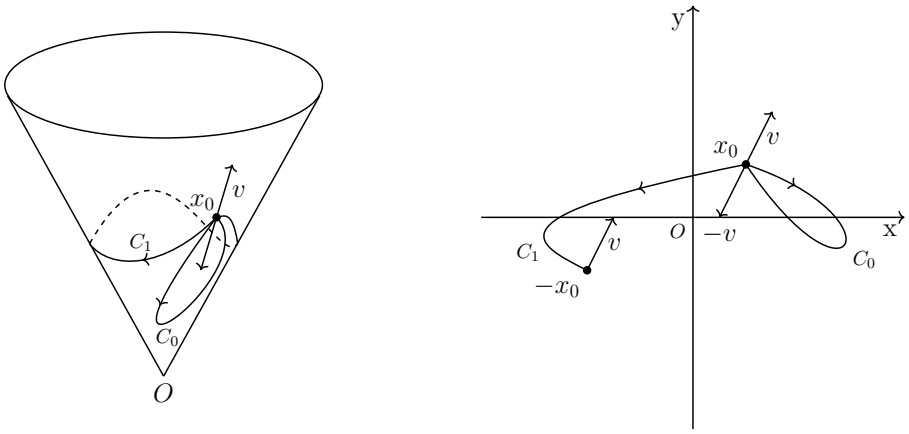

Figure 4.4: The relative space $r(2,2)$ (represented more accurately as a cone) and the covering space $\mathbb{R}^2 \setminus \{ 0 \}$. Two paths C_0 and C_1 are drawn, along with their lifts in $\mathbb{R}^2 \setminus \{ 0 \}$, and a vector v transported around the curves. The curve C_0 preserves v, while C_1 "flips" v when revolving around the vertex of the cone [4].

To finish off this intermezzo, we introduce the notion of a *section*, or *cross-section*.

Definition 4.4. *A section of a bundle $\widetilde{X}$ is a continuous map*

$$s : X \to \widetilde{X}$$

satisfying

$$p \circ s = \mathrm{id}_X$$

Effectively, the section "undoes" what the projection map does. In the case of a vector bundle, this means that every point in the base space gets assigned a vector in the fiber along with it, effectively giving us a vector field.

4.2.2 Constructing Anyons

Now that we have our mathematical background in order, we will consider the constructions by Leinaas and Myrheim [4] and that of Wilczek [2] alongside each other. In his article, Wilczek actually constructs multiple systems, one of which is a single-anyon system, and another is a two-anyon system. The former is physically less relevant, since it does not make much sense to talk about the statistics of a single particle, but it is simpler, and interesting nonetheless. Firstly, we will study the "abstract" construction by Leinaas and Myrheim alongside this single-anyon "physical" construction by Wilczek, in order to make the similarities more clear. Then we will look at the two-anyon system.

In the physical setup the starting point will be a particle with charge q orbiting an infinitely long solenoid on the z-axis with flux Φ, see Figure 4.5. Note that the loops in this setup are in fact equivalent to those in the once-punctured plane $\mathbb{R}^2 \setminus \{ 0 \}$. After all, they can all be continuously transformed to lie in this plane, and they cannot be "homotoped" around the solenoid (the "puncture"). In this setup, there is an azimuthal vector potential

$$\vec{A} = \frac{\Phi}{2\pi r}\hat{\varphi}$$

from the solenoid.

In the abstract setup we start with a given configuration space, and for each point x in this space we introduce a one-dimensional Hilbert space h_x. This space

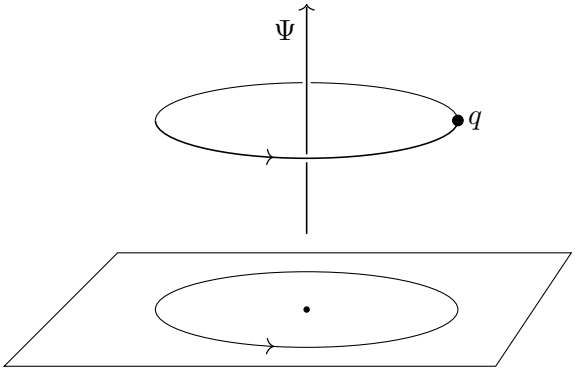

Figure 4.5: The physical setup used to describe the construction of a single anyon. It is depicted how the fundamental group of this space corresponds to that of $\mathbb{R}^2 \setminus \{ 0 \}$.

h_x is then the fiber of the bundle that describes the global state. Locally, we assume that the state of the system is described by the section $\Psi(x) \in h_x$. If we pick χ_x as a basis for h_x, then

$$\Psi(x) = \psi(x)\chi_x$$

for some complex valued function $\psi(x)$. In this way, we have constructed the fiber bundle that will give rise to specific gauge transformations. The function ψ depends on the choice of the basis vectors χ_x, and transforms with gauge transformations of the second kind when this basis changes:

$$\psi(x) \to \psi'(x) = e^{i\phi(x)}\psi(x) \tag{4.11}$$

for some function $\phi(x)$.

In the physical setup we perform a familiar gauge transformation, the same one that can be used to derive the Aharonov-Bohm effect [9]. We set

$$\vec{A}' = \vec{A} - \vec{\nabla}\Lambda, \quad \Lambda = \frac{\Phi\varphi}{2\pi}.$$

This causes the vector potential to be zero everywhere except the origin. This transformation corresponds to a transformation of the basis vectors χ_x, and the wave functions transform along with this as

$$\psi(\varphi) \to \psi'(\varphi) = e^{iq\Lambda(\varphi)}\psi(\varphi) = e^{iq\frac{\Phi\varphi}{2\pi}}\psi(\varphi).$$

By symmetry, ψ only depends on the azimuthal angle. Note that this turns $\psi'(\varphi)$ into a multi-valued function, since Λ is not 2π-periodic:

$$\psi(\varphi + 2\pi) = e^{iq\Phi}\psi(\varphi). \tag{4.12}$$

In the abstract setup we can also find this multi-valued nature of the wave functions. To see this, we observe the parallel displacement of the fibers h_x, and thereby of the state vectors. Denote the parallel displacement as a linear operator

$$P(x', x) : h_x \to h_{x'},$$

which transports each vector in the fiber h_x along a continuous curve from x to x' in the configuration space into a vector in the fiber $h_{x'}$ (along a horizontal lift of that curve!). Note that this transport may depend on the curve between x and x'. We may assume, though, that infinitesimal displacement from x to $x + \mathrm{d}x$ is uniquely defined, and unitary. An argument for uniqueness is that we are displacing by an infinitesimal

length, so as long as we stay within a small section, any choice of curve would give the same results. Unitariness follows essentially from the idea of parallel transport, as it will always conserve the inner product. A simple way of convincing yourself of this is by considering what happens to the inner product when transporting vectors around a sphere, see Figure 4.3.

Recalling the parallel transport equation (4.10), or a form of this that Leinaas and Myrheim refer to as the rule of infinitesimal displacement, we get

$$P(x + \mathrm{d}x, x)\chi_x = (1 + i\mathrm{d}x_k b_k(x))\chi_{x+\mathrm{d}x}, \tag{4.13}$$

using Einstein's summation convention. This corresponds to a gauge invariant differentiation operator

$$D_k = \frac{\partial}{\partial x_k} - ib_k(x). \tag{4.14}$$

Here, the functions b_k correspond to the dynamics of the system, and is referred to as the "gauge potential". The quantity

$$f_{kl} = i[D_k, D_l] = \frac{\partial b_l}{\partial x_k} - \frac{\partial b_k}{\partial x_l} \tag{4.15}$$

measures the noncommutativity of the components of the gauge-invariant differentiation, and essentially describes how curved our space is (in a flat space, with no gauge potential, this would be 0, and the covariant derivative becomes simply the partial derivative).

In the physical setup the gauge potential we mentioned corresponds directly with the vector potential A, and the covariant derivative is given by

$$D_k = \frac{\partial}{\partial x_k} - iqA_k.$$

We can in fact see more clearly what the covariant derivative entails in the physical setup. After a gauge transformation of $A_k \to A'_k$ and $\psi \to \psi'$, one can compute that

$$D'_k\psi' = e^{iq\Lambda}D_k\psi,$$

essentially saying that the covariant derivative of a transformed system is the transform of the covariant derivative, or in other words: it is preserved when moving along the bundle. The functions b_k are given by qA_k, and the commutators f_{kl} correspond to

$$f_{kl} = q\left(\frac{\partial A_l}{\partial x_k} - \frac{\partial A_k}{\partial x_l}\right) = qF_{kl},$$

where the F_{kl} are the elements of the electromagnetic field tensor.

In the abstract setup we do not want the functions b_k, corresponding to the vector potential, to describe a force field. So we assume that $f_{kl} = 0$ for all x except the singularity. This makes it so that a vector $\Psi \in h_x$ does not change when parallel transported around a closed curve not encircling the singularity. This follows from the Stoke's theorem. When transported m times around the singularity though, the wave function Ψ will be transformed into $P_x^m\Psi$, where P_x is a linear, unitary operator (unitary because we can assume that $P(x', x)$ is unitary). Since the Hilbert spaces h_x, where $\Psi(x)$ lies, is one-dimensional, P_x will just be a phase factor

$$P_x = e^{i\xi}.$$

Since

$$P_{x'} = P(x', x)P_xP(x', x)^{-1} = e^{i\xi},$$

the parameter ξ must not depend on the position x, and is therefore characteristic for the system itself. To obtain the beforementioned multi-valued nature of the wave function, we may choose χ_x in such a way that $b_k = 0$. This is precisely what we did with the gauge Λ in the physical setup. We can choose a basis vector χ_x at some point x and define the basis vectors at all other points as parallel transport of this basis vector, making it so that all basis vectors

$$\chi_x, e^{\pm i\xi}\chi_x, e^{\pm 2i\xi}\chi_x, \dots$$

exist at the point x, giving us the multi-valued nature of the wave function we found in the physical setup. With the operator P_x we can conclude that our wave functions must meet certain (unusual) boundary conditions, namely

$$\psi(\varphi + 2\pi) = e^{i\xi}\psi(\varphi). \tag{4.16}$$

In the physical setup we find that our allowed wave functions have

$$\psi(\varphi) \propto e^{il_z\varphi} \quad \text{with} \quad l_z = \text{integer} + \frac{q\Phi}{2\pi},$$

where the l_z show the spectrum of orbital angular momenta, in order to comply with our boundary condition (4.12).

The difference with the "normal" angular momentum values of integer l_z stems from the fact that in a 2D setup, there is *only* l_z, even though z in this case does not mean much physically. In the 3D setup, there are three components to the angular momentum, with commutation relations imposed on the operators. These are the same relations that are on the corresponding rotation group SO(3) of rotations in 3D space, a non-abelian, three dimensional group, see for example [15, Section 8.2.3]. In the 2D case, there are no restrictions, as the corresponding rotation group is SO(2), a one dimensional, abelian group.

Two anyons

Wilczek [2] also provides a physical construction for two anyons, in a similar setup. We consider two identical particles. In our setup, we consider the electrostatic forces small, and treat them as perturbation. We can define the wave function of our system Ψ as a function of center-of-mass coordinates R, θ and relative coordinates r, φ. This gives us a similar boundary condition as (4.16):

$$\Psi(R, \theta, r, \varphi + 2\pi) = e^{4\pi i\Delta}\Psi(R, \theta, r, \varphi) \tag{4.17}$$

with $\Delta = \frac{q\Phi}{2\pi}$ the angular momentum. Note that the difference with (4.16) is only a factor 2 in the change of phase. This is related to the fact that a loop of the two particles can be seen as the double exchange of the two [9, Section 3.2.6]. Since the particles are identical, a change of φ by π results in our original system, and we find that

$$\Psi(R, \theta, r, \varphi + \pi) = \pm e^{2\pi i\Delta}\Psi(R, \theta, r, \varphi). \tag{4.18}$$

Depending on whether our original particles were bosonic (+) or fermionic (−). In the case of bosonic particles, this results in boson statistics for $\Delta = 0$ and fermion statistics for $\Delta = \frac{1}{2}$, and anyon statistics for any value inbetween.

Harmonic Oscillator

We have seen the anyonic nature of the system in the phase of the wavefunction, and in the angular momenta of the system, but we can also find it in the allowed energies of the system. For this, we use a slightly different approach in the abstract setup. We again consider a two-particle system in 2D. In the relative space, the free particle Hamiltonian in polar coordinates reads

$$H = -\frac{\hbar^2}{m}\left(\frac{\partial^2}{\partial r^2} + \frac{1}{r}\frac{\partial}{\partial r} + \frac{4}{r^2}\frac{\partial^2}{\partial \varphi^2}\right).$$

We ignore the center of mass coordinate of the system. In the other approach, define the single-valued wavefunction

$$\psi'(r,\varphi) = e^{-i\frac{\xi}{2\pi}\varphi}\psi(r,\varphi). \tag{4.19}$$

We transform the Hamiltonian as

$$H' = e^{-i\frac{\xi}{2\pi}\varphi}He^{i\frac{\xi}{2\pi}\varphi} = -\frac{\hbar^2}{m}\left(\frac{\partial^2}{\partial r^2} + \frac{1}{r}\frac{\partial}{\partial r} + \frac{4}{r^2}\left(\frac{\partial}{\partial \varphi} + i\frac{\xi}{2\pi}\right)^2\right) \tag{4.20}$$

and note that ψ' is indeed a solution. We use a similar setup as before, but add a harmonic oscillator potential $V(r) = \frac{1}{4}m\omega^2 r^2$. The eigenfunctions of our new Hamiltonian $H' + V$ are

$$\psi'(r,\varphi) = e^{il\varphi}R(r) \tag{4.21}$$

for integer l. The radial function is determined by

$$\left(\frac{\partial^2}{\partial r^2} + \frac{1}{r}\frac{\partial}{\partial r} + \frac{4}{r^2}\left(l + \frac{\xi}{2\pi}\right)^2 - \frac{1}{4}\frac{m^2\omega^2}{\hbar^2}r^2 + \frac{mE}{\hbar^2}\right)R(r) = 0. \tag{4.22}$$

which is the ordinary radial equation, except with $l + \frac{\xi}{2\pi}$ instead of l. The result of this is that the allowed energies become

$$E = 2\hbar\omega\left(n + \left|l + \frac{\xi}{2\pi}\right| + \frac{1}{2}\right),$$

with $n = 0, 1, 2, \ldots$. This gives us the bosonic case for $\xi = 0$ and the fermionic case for $\xi = \pi$, as expected.

4.3 Anyons in Experiments

We have now seen the theoretical description of anyons, but they have been observed in practice as well. One major phenomenon where anyons show up is the *Fractional Quantum Hall Effect* (FQHE). I will describe this along [18], where David Tong gives a very clear derivation of the effect. We will first introduce the classical Hall effect, then discuss the Integer Quantum Hall effect, and finally the Fractional Quantum Hall Effect.

The classical Hall effect is the production of a voltage across a conducting plate, perpendicular to a current through the plate and an applied magnetic field perpendicular to the plate, see Figure 4.6. Classically, we could think of the magnetic field causing electrons to deflect off to one side, accumulating charge and creating an electric field causing an equilibrium. This induced electric field corresponds to the Hall voltage.

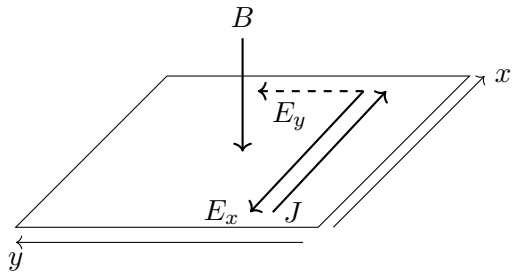

Figure 4.6: A setup where the Hall effect can be observed. Initially, a current with current density J flows through the plate, with a downwards magnetic field of strength B perpendicular to the plate and an electric field E_x across it. This causes an induced electric field E_y across the plate, and an associated voltage and resistivity.

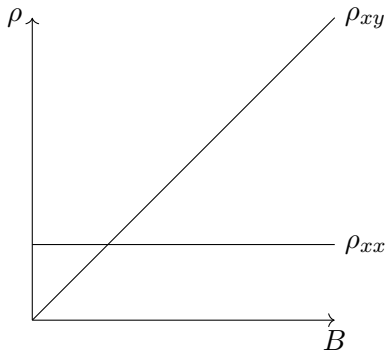

Figure 4.7: A sketch of what the Hall resistivity looks like in a classical picture.

A quantity that we will be looking at a bit more is the Hall resistivity. The resistivity is a tensor ρ defined as

$$\rho = \begin{pmatrix} \rho_{xx} & \rho_{xy} \\ -\rho_{xy} & \rho_{xx} \end{pmatrix} = \sigma^{-1} \tag{4.23}$$

for isotropic systems. Here, σ is the conductivity tensor, relating the current density $\vec{J}$ and the electric field $\vec{E}$ as $\vec{J} = \sigma\vec{E}$. The ρ_{xy} term is the Hall resistivity. Classically, one can derive that

$$\rho_{xx} = \frac{m}{ne^2\tau} \qquad \rho_{xy} = \frac{B}{ne}, \tag{4.24}$$

see Section 4.3. Here, B is the strength of the applied magnetic field, n is the density of charge carriers, m the mass of a charge carrier, $-e$ the charge of a particle and τ the *scattering time*, which can be thought of as the average time between collisions of charge carriers with for example impurities. A full derivation can be found in [18, Chapter 1.2].

4.3.1 The Integer Quantum Hall Effect

On very clean samples (plates), with strong magnetic fields and low temperatures, the Hall resistivity showed its quantized nature. This is known as the Integer Quantum Hall Effect (IQHE). The classical view of charge accumulating on one side no longer holds. Instead, the charge carriers move in circles in the plate (except at the edges, where they "bounce off" and move along the edge: the so called *edge modes*, see Figure 4.9).

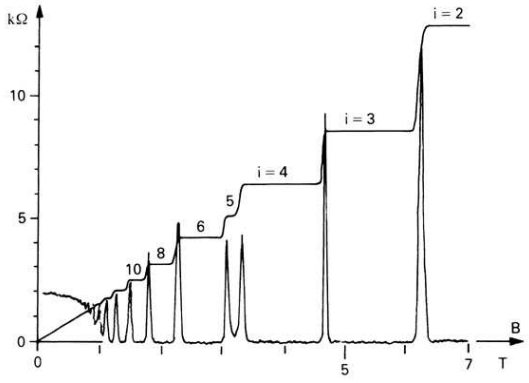

Figure 4.8: The IQHE. The vertical axis denotes the resistivity. The "steps" are the Hall resistivity ρ_{xy}, while the other line is the longitudinal resistivity ρ_{xx}. Classically, one would expect ρ_{xy} to be a line, and ρ_{xx} to be constant. Image extracted from [18].

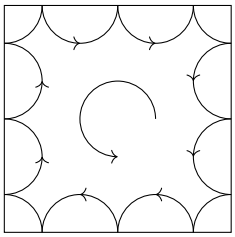

Figure 4.9: A sketch of what edge modes look like.

The resistivity components show quantized behavior, as can be seen in Figure 4.8. In the middle of the plateaus, the Hall resistivity takes the values

$$\rho_{xy} = \frac{2\pi\hbar}{e^2}\frac{1}{\nu} \qquad \nu \in \mathbb{Z} \tag{4.25}$$

A simple approach for explaining this value is observing ν fully filled Landau levels, and considering every single particle state, denoted $|\psi_{n,k}\rangle$, as a translation relative to the origin (in the middle of the plate), since all of the states should be the same motion.

For particles in a magnetic field, the Hamiltonian is given by

$$H = \frac{1}{2m}(\vec{p} + e\vec{A})^2. \tag{4.26}$$

It is known that the energies are quantized as

$$E_\nu = \hbar\omega_c\left(\nu - \frac{1}{2}\right) \tag{4.27}$$

where ν is a positive integer, and ω_c is the *cyclotron frequency*

$$\omega_c = \frac{eB}{m}. \tag{4.28}$$

These energy levels, known as *Landau levels*, are hugely degenerate. In fact, every level can house $\mathcal{N}$ particles, with

$$\mathcal{N} = \frac{AB}{\Phi_0}, \qquad \Phi_0 = \frac{2\pi\hbar}{e} \tag{4.29}$$

and A being the area of the plate. The quantity Φ_0 is known as the *flux quantum*. It can be thought of as the amount of flux contained in an area of $2\pi l_B^2$, where l_B is the *magnetic length*

$$l_B = \sqrt{\frac{\hbar}{eB}}, \tag{4.30}$$

the length scale at which quantum effects are important in a magnetic field. The degeneracy is lifted somewhat when adding an electric field $E\hat{x}$, turning the Hamiltonian into

$$H = \frac{1}{2m}(\vec{p} + e\vec{A})^2 - eEx. \tag{4.31}$$

This also results in an extra term added to E_ν, linear in k.

For the Hamiltonian (4.31) we can choose a convenient gauge for the vector potential $\vec{A}$. In this case, the vector potential is chosen as the *Landau gauge*

$$\vec{A} = -xB\hat{y}.$$

The sign comes from the fact that the magnetic field points downwards. The wavefunctions corresponding to this system (in this chosen gauge) are

$$\psi_{n,k} = e^{-iky} H_n(x - mE/eB^2 + kl_B^2) e^{-(x - mE/eB^2 + kl_B^2)^2/2lB^2}, \tag{4.32}$$

where H_n are the Hermite polynomials, as in the harmonic oscillator. They are sharply localized around

$$x = mE/eB^2 - kl_B^2. \tag{4.33}$$

The mE/eB^2 in this expression is merely a small uniform correction. The canonical momentum (note, not the mechanical momentum) of a particle in this system is given by

$$m\dot{\vec{x}} = \vec{p} + e\vec{A}.$$

For the current in the y-direction, this gives us

$$\begin{aligned} I_y = -e\dot{y} &= -\frac{e}{m}\sum_{n=1}^{\nu}\sum_k \langle\psi_{n,k}| - i\hbar\frac{\partial}{\partial y} - exB|\psi_{n,k}\rangle \\ &= \frac{e}{m}\sum_{n=1}^{\nu}\sum_k \langle\psi_{n,k}|\hbar k + exB|\psi_{n,k}\rangle\,. \end{aligned}$$

The $\hbar k$ term comes from the shape of the wavefunctions $\psi_{n,k}$, recalling (4.32). The second term calculates the expected value $\langle x\rangle$. From the localization of the wave functions, we find

$$I_y = e\nu\sum_k \frac{E}{B} = e\frac{E}{B}\mathcal{N} = AJ_y,$$

since the sum over k gives us simply the number of electrons in one Landau level. This in turn gives

$$E = \rho_{xy}J_y = \rho_{xy}\cdot\frac{e\nu E}{\Phi_0},$$

as expected.

This does not capture the edge modes mentioned earlier though, as well as disregarding all cases where the "degeneracy lifted" Landau levels are partially filled. A way of resolving this first point is by modelling the sample as having a potential with steep edges on the sides instead, see Figure 4.10.

Accounting for the edge modes in this way will not change anything about the results so far, as long as the Fermi level is inbetween two Landau levels. Now what

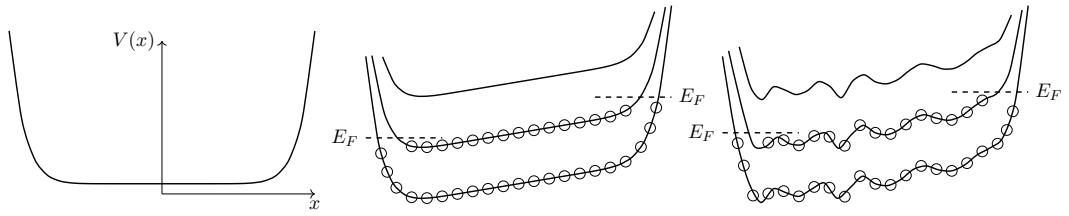

Figure 4.10: A sketch of the potential used to model the edge modes. In the middle, Landau levels along with the Fermi-level E_F are shown. The small circles represent occupied states. The slant in the Landau levels and the difference in the Fermi-level on the left and right side is because of the applied electric field in the x direction, and the potential associated with it. On the right side, a random potential representing the disorder is added, and the Landau levels are shown [18, Chapter 2].

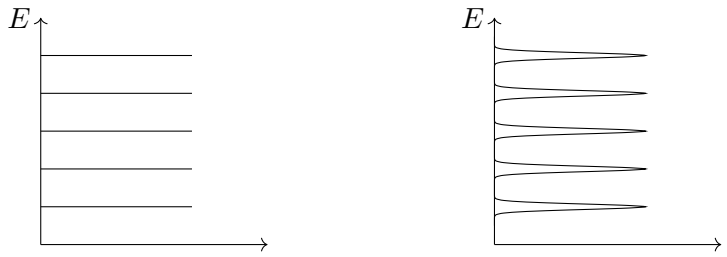

Figure 4.11: The density of states in the Landau levels with (left) and without (right) degeneracy [18, Figures 16 and 17].

happens when a Landau level (with its degeneracy lifted) is partially filled? It turns out that even though the plate is clean, the IQHE still occurs because the plates are not perfect, but just clean *enough*. Essentially, the disorder in the plate adds a random potential to that shown in Figure 4.10. As long as this random potential is much smaller than $\hbar\omega_c$, the gap between two Landau levels, this will not affect the quantized nature of the resistivity.

What happens is that this random potential adds some local maxima and minima to the sample. Particles are trapped around the minima and maxima, and will not contribute to the current. The states are *localized*. Lowering the magnetic field makes it so less states can occupy each Landau level. The Fermi level will rise, but the particles will start populating the localized states until a new Landau level is filled.

4.3.2 The Fractional Quantum Hall Effect

The phenomenon where anyons really play a role is in the Fractional Quantum Hall Effect (FQHE). It turns out that the resistivity does not only have plateaus at integer filling fractions ν, but also at fractional ones [19]. On even cleaner samples, and extremely low temperatures and high magnetic fields, plateaus were first found at $\nu = \frac{1}{3}$ and $\nu = \frac{2}{3}$ at the lowest Landau level, and later for other filling fractions and in different Landau levels.

Laughlin was the first to present a theory about the FQHE, describing the states with filling fractions

$$\nu = \frac{1}{m} \tag{4.34}$$

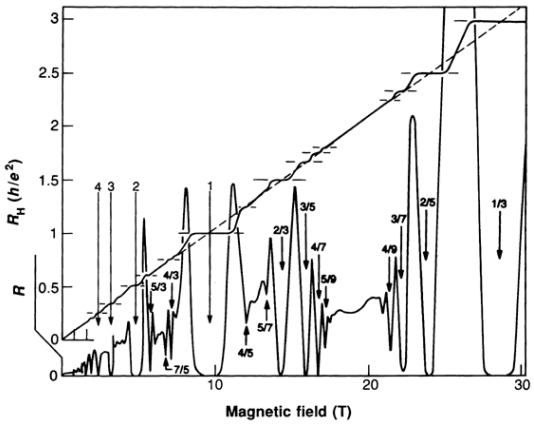

Figure 4.12: The Fractional Quantum Hall Effect. Image from [18].

for odd integers m [18]. He theorized a wave function, based on insight and guesswork:

$$\psi(z_i) = \prod_{i<j}(z_i - z_j)^m e^{-\sum_{i=1}^n |z_i|^2/4l_B^2}. \tag{4.35}$$

Here, the z_i represent the electron positions as complex numbers $z_i = x_i + iy_i$. This wavefunction was not perfect, but it showed more than 99% overlap with the true ground state. Hamiltonians can be found where this wavefunction is indeed an exact solution.

The most interesting part of this wavefunction is the "Jastrov factor"

$$\prod_{i<j}(z_i - z_j)^m.$$

It shows that m must be odd when observing electrons (which are fermions), to make the entire wavefunction odd under exchange of particles. States with even m can be seen as describing bosons. The meaning of m is quite complex, but can be interpreted for example as one plus the amount of flux quanta that is attached to each electron, turning them into "composite fermions"[9, Chapter 1], [20]. Note that there are $m(N-1)$ factors of z_1. By considering highest order monomial, we see that

$$z_1^{m(N-1)} e^{-\frac{|z_1|^2}{4l_B^2}} \tag{4.36}$$

is localized at a radius $R = \sqrt{m(N-1)}l_B$. This gives us an area for the "droplet" (since these wave functions describe more of a circular system) of particles $A \approx 2\pi m N l_B^2$, where we replace $N-1$ with N. The number of states in a full Landau level is $\frac{AB}{\Psi_0} = \frac{A}{2\pi l_B^2} \approx mN$. This argument shows that the filling fraction is indeed

$$\nu = \frac{1}{m}.$$

Now it can be shown that this state does in fact result in the desired resistivity. For the argument, see [18, Section 3.2.1].

We now consider excitations of the states discussed above. There are two types of charged excitations: *quasi-holes* and *quasi-particles*. To keep this thesis short and simple, we will only be considering quasi-holes. The wave function describing M quasi-holes at positions $\eta_i \in \mathbb{C}$, $i = 1, \ldots, M$ is

$$\psi_{M-\text{holes}}(z;\eta) = \prod_{j=1}^{M}\prod_{i=1}^{N}(z_i - \eta_j)\prod_{k<l}(z_k - z_l)^m e^{-\sum_{i=1}^n \frac{|z_i|^2}{4l_B^2}}. \tag{4.37}$$

Note how this describes the vanishing of the electron density at the holes η_i. An excitation like this for $m = 1$ can be seen as exciting a single particle, and creating a hole in the Fermi-sea that is the ground state. This hole will behave like a particle, but has no dynamics, and in our case has *fractional charge* $e^* = \frac{e}{m}$. A heuristic argument for this is that placing m quasi-holes on top of each other (so $\eta_i = \eta$ and $M = m$ in (4.37)) essentially gives us the Laughlin state with $z_{N+1} = \eta$. Except here η is a parameter, so m quasi-holes play the role of the absence of one electron.

A more formal argument for the fractional charge, and for the *fractional statistics* that we were looking for follows from a Berry phase when moving the quasi-holes around closed loops or exchanging them.

The Berry Phase

The Berry phase arises for a system with a Hamiltonian dependent not only on variables, but also on parameters λ, which we can write as

$$H(x_i; \lambda_j).$$

These λ_j are fixed by some external influence. We can change these parameters very slowly (adiabatically), and the Hamiltonian (and with that the eigenstates) changes too. The *adiabatic theorem* states that if we start with a system in a non-degenerate state, and make these adiabatic changes, the system will remain in this eigenstate. If we change these parameters in a way such that we return to the initial setup, the state will not change, except for a phase

$$|\psi\rangle \to e^{i\gamma} |\psi\rangle .$$

This phase is composed of two components, one comes from the time evolution, which is always there, and the other is the *Berry phase*.

This concept is very closely related to parallel transport. An example in classical mechanics is the *Foucault pendulum*, where the rotation of the earth causes the pendulum to gradualy change direction. In fact, carrying a Foucault pendulum around the earth in a way similar to Figure 4.3 would give it the exact same phase change as the vector carried around in the figure [21, Section 11.5].

The Berry phase can be calculated as

$$e^{i\gamma} = \exp\left(-i \oint_C \mathcal{A}_j \mathrm{d}\lambda_j\right) \tag{4.38}$$

where $\mathcal{A}_j$ is the *Berry connection*, defined as

$$\mathcal{A}_j = -i \langle n| \frac{\partial}{\partial \lambda_j} |n\rangle . \tag{4.39}$$

The state $|n\rangle$ is a reference state with a certain initial phase. The Berry connection is similar to other connections we discussed earlier. We can apply gauge transformations to the Berry connection for example. The freedom of choice of gauge in this case arises from the arbitrariness of the initial phase of the reference states $|n\rangle$ of the system.

Fractional Charge and Fractional Statistics

For our system of quasi-holes, we consider the normalized states

$$|\psi\rangle = \frac{1}{\sqrt{Z}} |\eta_1, \ldots, \eta_M\rangle , \tag{4.40}$$

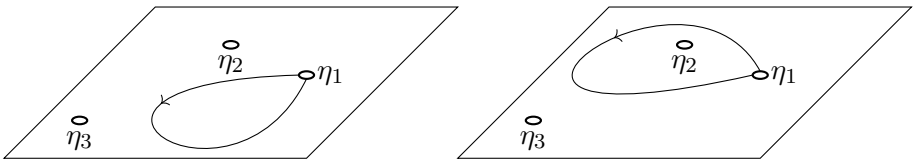

Figure 4.13: Loops to compute fractional charge (left) and fractional statistics (right) of quasi-holes [18, Figures 31 and 32].

where $|\eta_1, \ldots, \eta_M\rangle$ has wavefunction (4.37), and Z is a normalization factor dependent on the η_j. In our case, the parameters η_j are not real, and we consider the "holomorphic" and "anti-holomorphic" parameters η and $\overline{\eta}$ respectively. The holomorphic Berry connection is

$$\mathcal{A}_\eta(\eta, \overline{\eta}) = -i \langle\psi| \frac{\partial}{\partial \eta} |\psi\rangle = \frac{1}{2Z} \frac{\partial Z}{\partial \eta} - \frac{i}{Z} \langle\eta| \frac{\partial}{\partial \eta} |\eta\rangle = -\frac{i}{2} \frac{\partial \log(Z)}{\partial \eta}, \tag{4.41}$$

because $\frac{\partial Z}{\partial \eta} = \frac{\partial}{\partial \eta} \langle\eta|\eta\rangle = \langle\eta| \frac{\partial}{\partial \eta} |\eta\rangle$. The anti-holomorphic Berry connection is

$$\mathcal{A}_{\overline{\eta}} = +\frac{i}{2} \frac{\partial \log(Z)}{\partial \overline{\eta}}. \tag{4.42}$$

The exact expression for Z is not known, but an approximation can be found in [18, below Equation (3.24)]. Some analysis, also done in the referenced article, allows one to derive that

$$\mathcal{A}_{\eta_j} = -\frac{i}{2m} \sum_{j \neq i} \left(\frac{1}{\eta_i - \eta_j} \right) + \frac{i\overline{\eta}_j}{4ml_B^2} \quad \text{and} \quad \mathcal{A}_{\overline{\eta}_j} = +\frac{i}{2m} \sum_{j \neq i} \left(\frac{1}{\overline{\eta}_i - \overline{\eta}_j} \right) - \frac{i\eta_j}{4ml_B^2}, \tag{4.43}$$

if the holes do not get too close to each other.

To derive the fractional charge, we move a quasi-hole η_1 around a loop that does not enclose any other quasi-holes, see Figure 4.13. In that case, the first term of the Berry connection does not contribute to the phase (a well known result of complex analysis). The Berry phase is then given by

$$e^{i\gamma} = \exp\left(-i \oint_C \mathcal{A}_\eta \mathrm{d}\eta + \mathcal{A}_{\overline{\eta}} \mathrm{d}\overline{\eta} \right) = \exp\left(-i \oint_C \frac{i\overline{\eta}_j}{4ml_B^2} \mathrm{d}\eta - \frac{i\eta_j}{4ml_B^2} \mathrm{d}\overline{\eta} \right). \tag{4.44}$$

Stokes theorem gives us that

$$\oint_C \frac{i\overline{\eta}_j}{4ml_B^2} \mathrm{d}\eta = -\frac{1}{4ml_B^2} \cdot A = \frac{e\Phi_0}{2m\hbar} \cdot \frac{A}{2\pi l_B} = -\frac{e\Phi}{2m\hbar},$$

where Φ_0 is the flux quantum, defined as Equation (4.29), the flux through an area $2\pi l_B^2$, and Φ is the total flux through the area enclosed by C. The same thing can be done for the anti-holomorphic term, giving us the Berry phase

$$\gamma = \frac{e\Phi}{m\hbar}, \tag{4.45}$$

which is exactly the Aharonov-Bohm phase for a particle with charge

$$e^* = \frac{e}{m}.$$

More importantly though, we wish to look at the fractional statistics. For this, we choose a loop which *does* enclose another quasi-hole, see Figure 4.13. In this case, both terms contribute. The second term again gives the Aharonov-Bohm phase. The first term gives

$$\frac{1}{2m}\oint_C \frac{\mathrm{d}\eta_1}{\eta_1-\eta_2} = \frac{\pi i}{m},$$

for both $\mathcal{A}_\eta$ and $\mathcal{A}_\eta$, following from Cauchy's integral theorem. The sign is a combination of that in (4.38) and (4.44). Adding the term from the anti-holomorphic Berry connection gives us

$$e^{i\gamma} = e^{\frac{2\pi i}{m}}. \tag{4.46}$$

Note that this is for a rotation of one quasi-hole around another, and an exchange would give half this phase. This makes it so that for a fully filled Landau level ($m = 1$), the quasi-holes are fermions.

Chapter 5

Braided Monoidal Categories

Braid structures occur in other mathematical contexts as well. One of these is category theory, where there are braided structures called *braided monoidal categories*. Category theory studies a very generic abstraction of other mathematical structures in the form of *categories*. I will introduce some basic category theory along [22]. After this, we will be looking at monoidal categories, and finally braided monoidal categories. Finally, we will explore some interesting uses of braided monoidal categories.

5.1 Category Theory: A Short Introduction

Definition 5.1. *A* category *consists of:*

- *A directed graph with a set O of objects (the vertices) and a set A of arrows or morphisms (the edges);*
- *two functions* $\mathrm{dom} : A \to O$ *and* $\mathrm{cod} : A \to O$*, such that two arrows g, f are* composable *if* $\mathrm{dom}\, g = \mathrm{cod}\, f$*;*
- *and two additional functions*

$$\mathrm{id} : O \to A : c \mapsto \mathrm{id}_c, \tag{5.1}$$
$$\circ : A \times_O A \to A : (g, f) \mapsto g \circ f, \tag{5.2}$$

called the identity and composition.

Here, $A \times_O A$ denotes the set of composable arrows.

$$A \times_O A = \{\ (g, f) \mid g, f \in A, \mathrm{dom}\, g = \mathrm{cod}\, f\ \}$$

For the functions id *and* $\circ$ *the following must hold:*

$$\mathrm{dom}(\mathrm{id}\, a) = a = \mathrm{cod}(\mathrm{id}\, a) \tag{5.3}$$
$$\mathrm{dom}(g \circ f) = \mathrm{dom}\, f \tag{5.4}$$
$$\mathrm{cod}(g \circ f) = \mathrm{cod}\, g \tag{5.5}$$

for objects $a \in O$ and composable arrows $(g, f) \in A \times_O A$.

To distinguish between arrows *in* a category and objects *in* a category, we write

$$c \in C \quad \text{and} \quad f \text{ in } C$$

for objects and arrows respectively. We also write

$$\hom(b, c) = \{\ f \mid f \text{ in } C, \mathrm{dom}\, f = b, \mathrm{cod}\, f = c\ \} \tag{5.6}$$

for the *hom-set* of morphisms between objects b and c. Categories are often depicted as shown below

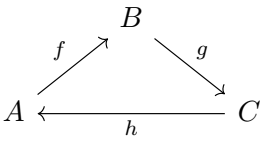

Some categories are given special names, like

- **Set**, the category with "small" sets as objects and functions between them as arrows;
- **Grp**, the category with "small" groups as objects and group homomorphisms as arrows;
- **Top**, the category of "small" toplogical spaces, with continuous functions as arrows;
- **Vect**(k), the category of "small" vector spaces over a field k, with linear maps as arrows;

and others. Small here means sets within a specific "universe", dependent on the context. Essentially all "small" sets are "all sets one cares to consider" [8, `Small set`].

Categories themselves may also admit morphisms between them, which we call *Functors*.

Definition 5.2. *A functor $T : C \to B$ between two categories C and B consists of two functions: the object function and the arrow function (both written T). These functions assign to each object $c \in C$ and each arrow f in C an object $Tc \in B$ and an arrow Tf in B respectively, in such a way that*

$$T(\mathrm{id}_c) = \mathrm{id}_{Tc} \quad \textit{and} \quad T(g \circ f) = Tg \circ Tf. \tag{5.7}$$

A simple example is the power set functor $\mathcal{P} : \mathbf{Set} \to \mathbf{Set}$, which takes sets to their powersets, and functions $f : X \to Y$ to $\mathcal{P}f : \mathcal{P}X \to \mathcal{P}Y$ sending each subset $S \subset X$ to its image $fS \subset Y$. It is easily verified that $\mathcal{P}$ satisfies the conditions (5.7).

We can construct the *product category* $B \times C$ for categories B and C as follows: an object of $B \times C$ is a pair of objects (b, c) with $b \in B$, $c \in C$. An arrow $(b, c) \to (b', c')$ is a pair of arrows $f : b \to b'$ and $g : c \to c'$. Composition is defined in the natural way as elementwise composition. We can define *projection* functors $P : B \times C \to B$ and $Q : B \times C \to C$ by simply taking the respective element of the object and arrow tuples. The product category between a category C and the category **2**, consisting of two objects $0, 1$ and one arrow from 0 to 1, can be depicted nicely:

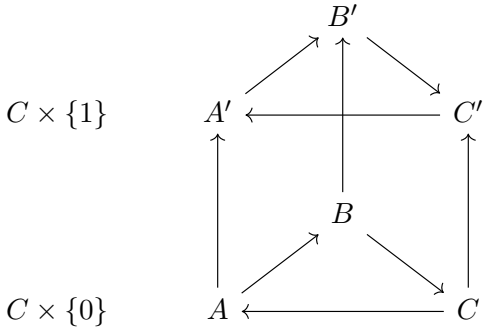

The last basic notion we need is that of *natural transformations*.

Definition 5.3. *Given two functors $S, T : C \to B$ for categories C and B, a natural transformation $\tau : S \to T$ is a function which assigns to each object of C an arrow $\tau_c = \tau c : Sc \to Tc$ of B, in such a way that the following diagram is commutative.*

$$\begin{array}{ccc} c & & Sc \xrightarrow{\tau c} Tc \\ {\scriptstyle f}\downarrow & & {\scriptstyle Sf}\downarrow \quad\quad \downarrow{\scriptstyle Tf} \\ c' & & Sc' \xrightarrow{\tau c'} Tc' \end{array}$$

One also says that $\tau_c : Sc \to Tc$ is *natural* in c.

5.2 Monoidal Categories

A logical next step to understanding braided monoidal categories is understanding monoidal categories. The definition is closely related to that of a *monoid*. A monoid is a set equipped with an associative binary operation and an identity element. One can think of this as a set with a multiplication or a product, essentially a group without the requirement of inverses. Similarly, we can define a *monoidal category*.

Definition 5.4. *A monoidal category (sometimes referred to as* tensor category*) is a category C equipped with [6, `Monoidal Category`]*

- *A functor $\otimes : C \times C \to C$ from the product category of C to itself, called the* tensor product*.*
- *An object $e \in C$.*
- *A natural isomorphism*

$$\alpha = \alpha_{a,b,c} : a \otimes (b \otimes c) \simeq (a \otimes b) \otimes c,$$

  for $a, b, c \in C$, called the associator*.*
- *A natural isomorphism*

$$\lambda = \lambda_x : e \otimes x \to x$$

  called the left unitor*, and*
- *A natural isomorphism*

$$\rho = \rho_x : x \otimes e \to x$$

  called the right unitor*.*

such that the following two kinds of diagrams commute: the triangle identity

$$\begin{array}{ccc} (x \otimes e) \otimes y & \xrightarrow{a_{x,e,y}} & x \otimes (e \otimes y) \\ & {\scriptstyle \rho_x \otimes \mathrm{id}_y} \searrow \quad \swarrow {\scriptstyle \mathrm{id}_x \otimes \lambda_y} & \\ & x \otimes y & \end{array}$$

and the pentagon identity

$$\begin{array}{ccccc} & & (w \otimes x) \otimes (y \otimes z) & & \\ & {\scriptstyle \alpha_{w\otimes x,y,z}} \swarrow & & \searrow {\scriptstyle \alpha_{w,x,y\otimes z}} & \\ ((w \otimes x) \otimes y) \otimes z & & & & w \otimes (x \otimes (y \otimes z)) \\ {\scriptstyle \alpha_{w,x,y}\otimes \mathrm{id}_z}\downarrow & & & & \uparrow{\scriptstyle \mathrm{id}_w \otimes \alpha_{x,y,z}} \\ (w \otimes (x \otimes y)) \otimes z & & \xrightarrow[\alpha_{w,x\otimes y,z}]{} & & w \otimes ((x \otimes y) \otimes z) \end{array}$$

A monoidal category is called *strict* when the associator and both the left and right unitor are identity morphisms.

Example 5.5. *An example of a monoidal category is the category of sets* **Set**, *with the cartesian product as tensor product, and any 1-element set as its unit.*

5.3 Braided Monoidal Categories

A braided monoidal category is a monoidal category with an added *braiding*: an isomorphism essentially describing how the tensor product commutes.

Definition 5.6. *A braided monoidal category is a monoidal category C, along with a family of isomorphisms called a* braiding $\gamma = \gamma_{a,b} : a \otimes b \simeq b \otimes a$, *natural in $a, b \in C$ such that the following two diagrams commute:*

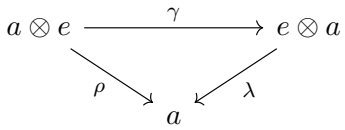

and the Hexagon Axiom *(the symbol $\otimes$ is omitted)*

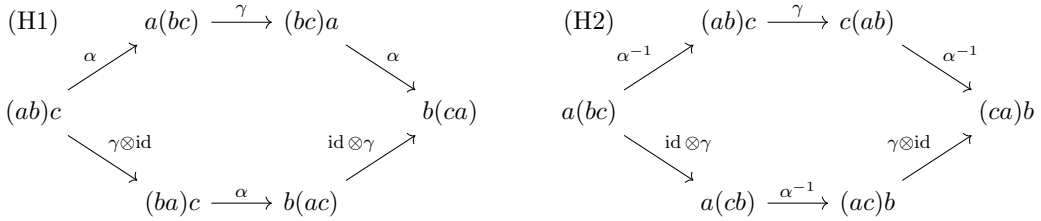

In the special case where $\gamma_{a,b} \circ \gamma_{b,a} = \mathrm{id}$, the braided monoidal category is called a *symmetric monoidal category.*

Example 5.7. *An example of a braided monoidal category is the category* $\mathbf{Vect}(k)$, *with the classic tensor product, and "the flip", associating $V \otimes W$ with $W \otimes V$, as braiding [23, Chapter 13]. This is in fact a symmetric monoidal category.*

5.3.1 The Braid Category

One, perhaps basic, example is that of the *braid category* $\mathbb{B}$. Braided monoidal categories, as well as the braid category itself were studied by Joyal and Street [3], but I will be following [23, Chapter 13] and [22, Chapter 11]. The braid category $\mathbb{B}$ may be defined as a category with the braid groups as objects, though often we simply choose the natural numbers. The arrows are the braids $n \to n$, $n \in B$. There are no arrows between two braid groups $n \neq m$.

This category is a (strict) monoidal category when we define $\otimes$ as the "addition" of braids, or simply "laying" one braid next to another, see Figure 5.1. The empty braid is the unit. We can then define the braiding $\gamma_{n,m}$ pictorially as seen on the left hand side in Figure 5.2, where $\gamma_{0,n} = \gamma_{n,0} = \mathrm{id}_n$. It can also be defined algebraically in terms of braid group generators σ_i as [23]

$$\gamma_{n,m} = (\sigma_m \sigma_{m-1} \dots \sigma_1)(\sigma_{m+1} \sigma_m \dots \sigma_2) \dots (\sigma_{m+n-1} \sigma_{m+n-2} \dots \sigma_n) \tag{5.8}$$

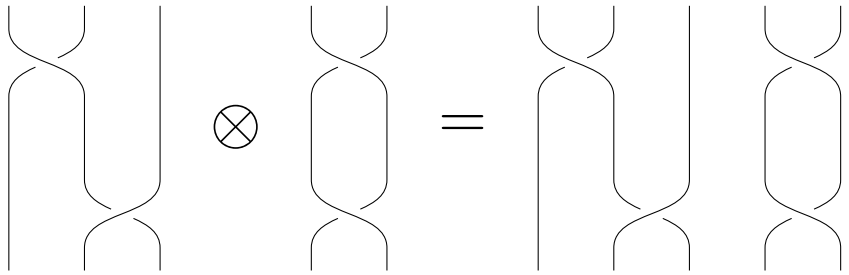

Figure 5.1: An illustration of the tensor product on the braid category $\mathbb{B}$.

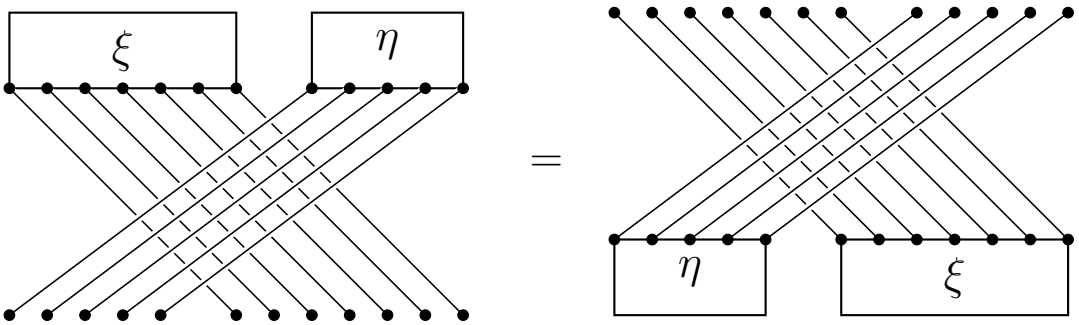

Figure 5.2: The left hand side shows the braiding $\gamma_{n,m}$ on the braid category $\mathbb{B}$ shown pictorially. The boxes ξ, η represent braids in $n = 7$ and $m = 5$ respectively. The right hand side shows the same braid, showing that $\gamma_{m,n}$ is indeed natural.

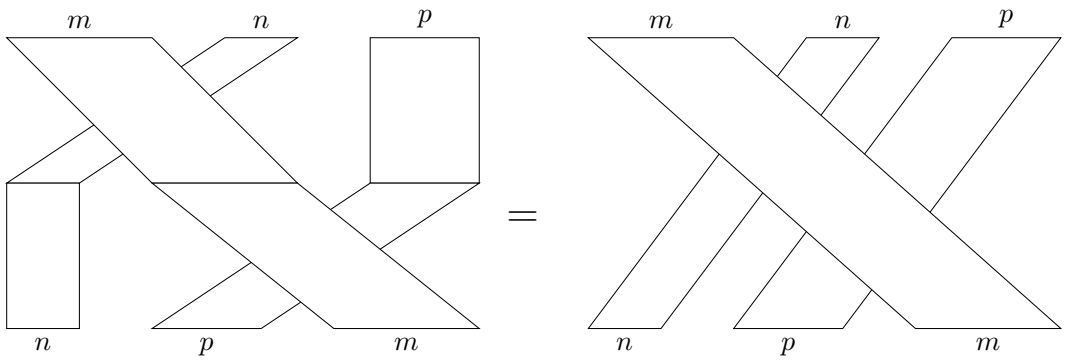

Figure 5.3: The first relation of the hexagon axiom (H1) shown pictorially for the braid category. The "lower path" in the hexagonal diagram corresponds to the left hand side of this figure, while the "upper path" corresponds to the right hand side. [3]

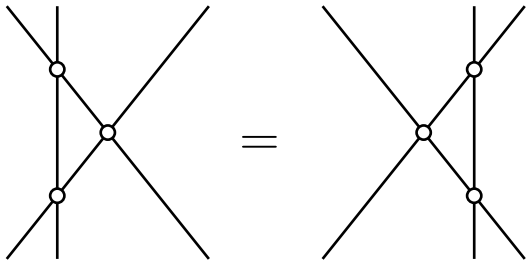

Figure 5.4: A visual representation of the Yang-Baxter equation (5.10).

Showing the naturality and the fulfillment of the hexagon axiom can again be done most easily pictorially. Naturality can be seen in Figure 5.2, which shows that the order of applying the braiding $\gamma_{m,n}$ and the braids $\xi \otimes \eta$ does indeed not matter. The first relation of the hexagon axiom (H1) can be pictorially verified, as seen in Figure 5.3. The other relation can be verified in a similar way. It can also be shown algebraically, but this would be a very long and not very exciting proof.

One important thing to note though, is that [23]

$$\sigma_i \text{ is represented by } \mathrm{id}_1^{\otimes(i-1)} \otimes \gamma_{1,1} \otimes \mathrm{id}_1^{\otimes(n-i-1)} \tag{5.9}$$

for any $i = 1, 2, \ldots, n$. Here $\mathrm{id}_1^{\otimes(n)}$ denotes $\mathrm{id}_1 \otimes \mathrm{id}_1 \otimes \ldots \otimes \mathrm{id}_1$, n times id_1 tensored with itself. In the case of the braid category, this seems like a fairly trivial result, but it suggests that if we find other braided monoidal categories (for example ones with $\mathbb{C}$-vector spaces as objects), we might find representations of the braid groups in the same way.

For example, consider Lemma X.6.8 from [23, Chapter X].

Lemma 5.8. *Let V be a vector space, and c a linear automorphism of $V \otimes V$, and $n > 1$ an integer. Then the linear automorphism c_i of $V^{\otimes n}$, for $1 \leq i < n$ defined as*

$$c_i = \begin{cases} c \otimes \mathrm{id}_{V^{\otimes(n-2)}} & \text{if } i = 1, \\ \mathrm{id}_{V^{\otimes(i-1)}} \otimes c \otimes \mathrm{id}_{V^{\otimes(n-i-1)}} & \text{if } 1 < i < n-1, \\ \mathrm{id}_{V^{\otimes(n-2)}} \otimes c & \text{if } i = n-1 \end{cases}$$

satisfies

$$c_i c_{i+1} c_i = c_{i+1} c_i c_{i+1}$$

if and only if c is a solution of the Yang-Baxter equation (5.10).

Note that the first braid relation (B1) is trivially satisfied by the c_i, simply from its construction.

The Yang-Baxter equation is an equation that was first come up with while studying scattering of particles and in studying models in statistical physics. The equation reads

$$(c \otimes \mathrm{id}_V)(\mathrm{id}_V \otimes c)(c \otimes \mathrm{id}_V) = (\mathrm{id}_V \otimes c)(c \otimes \mathrm{id}_V)(\mathrm{id}_V \otimes c). \tag{5.10}$$

It describes the scattering of particles, and says that when scattering three particles, it can be reduced to a two body problem. That it does not matter in what order the particles interact. This is often represented graphically as seen in Figure 5.4. One can construct a dodecagonal diagram that always commutes in braided monoidal categories, equivalent to precisely the Yang-Baxter equation when the monoidal category is strict [23, Theorem XIII.1.3]. If the monoidal category is not strict, one has to account for the associator. This, by the construction used in Lemma 5.8, shows that

the braiding on a strict braided monoidal category provides braid group representations on vector spaces in the way implied by Equation (5.9). We can come up with some basic examples starting from braided monoidal categories.

Example 5.9. *The category* $\mathbf{Vect}(k)$ *is a braided monoidal category with the classic tensor product and "the flip" as braiding.*

This example is symmetric, so the result will not be very exciting, but it is a good example nonetheless. The matrices that represent "the flip" $\tau_{V,W} : V \otimes W \to W \otimes V$ are

$$\begin{pmatrix} 0 & I_W \\ I_V & 0 \end{pmatrix}.$$

Similar to Equation (5.9), we find that

$$\sigma_i \in B_n \text{ is represented by } \begin{pmatrix} I_{i-1} & 0 & 0 & 0 \\ 0 & 0 & 1 & 0 \\ 0 & 1 & 0 & 0 \\ 0 & 0 & 0 & I_{n-i-1} \end{pmatrix}$$

using the braiding on a one-dimensional vector space, similar to how we used 1 in Equation (5.9). We could have used and n-dimensional vector space, but this would simply replace all I_k by I_{nk} and 1 by I_n. Note that squaring this matrix yields I_n, so this is in fact a representation of the symmetric group S_n as well.

Example 5.10. *For a commutative ring* R*, let* V_0 *be the category* $\mathbf{GMod}_R$ *of graded* R*-modules with tensor product given by*

$$(A \otimes B)_n = \sum_{p+q=n} A_p \otimes_R B_q.$$

Braidings on this monoidal structure on $\mathbf{GMod}_R$ *are given by*

$$c(x \otimes y) = k^{pq}(y \otimes x) \text{ where } x \in A_p, y \in B_q$$

for some $k \in R$*.*

This is an example presented by Joyal and Street [3]. A graded module is a module M over a ring R such that

$$M = \bigoplus_{n=0}^{\infty} M_n$$

An example of a graded module is a "graded vector space" over a field (where the field has trivial braiding $R_i = 0$ for $i \geq 1$), defined in the same way [8, `Graded ring`]. Another example is

$$M := R[x]/x^2$$

over a ring R. Here, we have $M_0 = R$, $M_1 = R[x]_1$ and $M_n = 0$ for $n > 1$. We can see the tensor product as

$$M \otimes M \cong R[x, y]/(x^2, y^2)$$

and the braiding maps

$$c : a + bx + cy + dxy \mapsto a + kby + kcx + k^2 dxy.$$

We can derive matrices representing the braid group from this braiding. We consider B_3, with generators σ_1 and σ_2 corresponding to $c \otimes \mathrm{id}$ and $\mathrm{id} \times c$ (acting on $M \otimes M \otimes M \cong R[x,y,z]/(x^2,y^2,z^2)$). These maps can be represented as

$$\begin{pmatrix} 1 & 0 & 0 & 0 & 0 & 0 & 0 & 0 \\ 0 & 0 & k & 0 & 0 & 0 & 0 & 0 \\ 0 & k & 0 & 0 & 0 & 0 & 0 & 0 \\ 0 & 0 & 0 & k^2 & 0 & 0 & 0 & 0 \\ 0 & 0 & 0 & 0 & 1 & 0 & 0 & 0 \\ 0 & 0 & 0 & 0 & 0 & 0 & k & 0 \\ 0 & 0 & 0 & 0 & 0 & k & 0 & 0 \\ 0 & 0 & 0 & 0 & 0 & 0 & 0 & k^2 \end{pmatrix} \quad \text{and} \quad \begin{pmatrix} 1 & 0 & 0 & 0 & 0 & 0 & 0 & 0 \\ 0 & 1 & 0 & 0 & 0 & 0 & 0 & 0 \\ 0 & 0 & 0 & 0 & k & 0 & 0 & 0 \\ 0 & 0 & 0 & 0 & 0 & k & 0 & 0 \\ 0 & 0 & k & 0 & 0 & 0 & 0 & 0 \\ 0 & 0 & 0 & k & 0 & 0 & 0 & 0 \\ 0 & 0 & 0 & 0 & 0 & 0 & k^2 & 0 \\ 0 & 0 & 0 & 0 & 0 & 0 & 0 & k^2 \end{pmatrix}. \tag{5.11}$$

respectively, on the basis $\{\, 1, x, y, xy, z, xz, yz, xyz \,\}$. For braid groups on more strands, the matrices become larger, but can be derived in the same way. Note that if we consider the ring R as a graded module over itself (with trivial braiding $M_l = R$, $M_i = 0$ for $i \neq l$), we get an even simpler, yet not necessarily symmetric braiding, where

$$\sigma_i \in B_n \text{ is represented by } \begin{pmatrix} I_{i-1} & 0 & 0 & 0 \\ 0 & 0 & k^{2l} & 0 \\ 0 & k^{2l} & 0 & 0 \\ 0 & 0 & 0 & I_{n-i-1} \end{pmatrix}. \tag{5.12}$$

Note that these braidings become symmetric when $k^2 = 1$.

Another way to find braid group representations is by starting from a *braided bialgebra*. I will not provide the precise definition here, but it can be found in [10, Chapter 5]. Essentially, from a braided bialgebra A, one can construct the braided monoidal category $A-\mathbf{Mod}$ of left A-modules. The braiding on this category can be found from a "universal R-matrix" in $A \otimes A$. Then, one can construct braid group representations in the way described before. Jackson [10] provides examples of this in his thesis, showing how the Burau representation and the Lawrence-Krammer-Bigelow representation can be derived from the braided bialgebra $U_q(\mathfrak{sl}_2)$, called the "quantum algebra".

Chapter 6

Outlook

There is more to braid groups and their applications than we were able to look at in this thesis. We have seen different representations like the Burau representation, the Lawrence-Krammer-Bigelow representation and the braid group as fundamental group of the configuration space of particles moving around on the plane. Regarding representations, one could study these representations in more detail, or study braided bialgebras and how one obtains braid group representations from those, for example see [10]. Braided bialgebras have another connection with physics, namely with quantum groups, used to study certain quantum systems [23, Chapter 8]. Another, related field of study might be that of knots and links, see for example [1]. One can obtain knots from braids and vice versa (Alexander's Theorem). One can also construct isotopy invariants of knots and links using the theory of braided structures [23].

We studied anyons, particles following statistics different from bosons and fermions, and how they arise from the theory of braid groups. There is also a lot more to explore regarding physics and anyons. For example the theorized "non-abelian" anyons, where one must consider higher dimensional braid group representations, instead of the one-dimensional ones we looked at in Chapter 4. One could also look at composite fermions, and the mathematical theory behind those, see for example [9, Chapter 4]. Or one could look into practical applications of (non-abelian) anyons, for example in topological quantum computing, researched by Microsoft. Another interesting tangential topic regarding anyons is the realization of anyons by other means, even regardless of the spatial dimension, for example using Haldane's generalized exclusion principle [24].

Appendix A

Fadell's Exact Sequence

In this appendix, we wish to prove Theorem 2.20. We use the same notation as in Section 2.5. Let us recall what the theorem of interest stated:

Theorem 2.20. *There exist homomorphisms ι_* and π_* such that the following sequence of groups is exact:*

$$\{\,1\,\} \longrightarrow \pi_1(F_{N-1,1}) \xrightarrow{\iota_*} \pi_1(F_N) \xrightarrow{\pi_*} \pi_1(F_{N-1}) \longrightarrow \{\,1\,\}$$

To prove this, we want to look at a *locally trivial fibration* of the space F_N, induced by a map from F_N to F_{N-1}.

Definition A.1. *A* locally trivial fibration *is a continuous surjective map $\pi : \tilde{X} \to X$ with a* fibre *F if for every $x \in X$ there exists a neighborhood $U \subset X$ of x and a homeomorphism $\theta : U \times F \to \pi^{-1}(U)$ such that $\pi \circ \theta$ is the projection on the first factor U. [25]*

For example, in the visual example from Figure 2.4, the map p is a locally trivial fibration.

To prove the theorem of interest, we prove the following result, which is a specific case of a theorem by Fadell and Neuwirth [26]. To avoid any confusion, I will write $F_{0,N}$ for F_N, which is in fact equivalent.

Theorem A.2. *Let $\pi : F_{0,N} \to F_{0,N-1}$ be defined by*

$$\pi(z_1, z_2, \ldots, z_N) = (z_1, z_2, \ldots, z_{N-1}) \tag{A.1}$$

Then π is a locally trivial fibration over the base space $F_{0,N-1}$ with fibre $F_{N-1,1}$.

We can actually get a bit of an idea for this by looking at $\pi^{-1}(z)$ for $z \in F_{0,N-1}$. The pullback of z is the set of points

$$\pi^{-1}(z_1, z_2, \ldots, z_{N-1}) = \\ \left\{\, (z_1, z_2, \ldots, z_{N-1}, z_N) \;\middle|\; z_N \in \mathbb{R}^2, z_N \neq z_i \text{ for } i = 1, 2, \ldots, N-1 \,\right\}.$$

We can see this as if we are simply trying to place a point z_N in $\mathbb{R}^2$ with $N-1$ punctures $z_1, \ldots, z_{N-1}$. The idea is to then find a homeomorphism that takes the z_i with $i = 1, \ldots, N-1$ to the punctures. The proof is an adaptation of the proof in [26].

Proof. Fix a point $x_0 = (x_{0,1}, \ldots, x_{0,N-1}) \in F_{0,N-1}$, and set

$$H_{N-1} = \left\{ z_0, z_1, \ldots, z_{N-1} \;\middle|\; z_i \in \mathbb{R}^2, z_i \neq z_j \text{ if } i \neq j \right\}$$

for distinct points z_i. Recall that

$$F_{N-1,1} = \mathbb{R}^2 \setminus H_{N-1}.$$

Take an open neighborhood of the form U^{N-1}, with $U \subset \mathbb{R}^2$ open, around x_0 in $F_{0,N-1}$. Define a homeomorphism

$$\theta(x, y) : U^{N-1} \times \overline{U} \to \overline{U}$$

such that, if we write $\theta_{(x_1,x_2,\ldots,x_{N-1})}(y) = \theta(x, y)$, we have

(i) $\theta_x : \overline{U} \to \overline{U}$ is a homeomorphism having $\partial\overline{U}$ fixed.

(ii) $\theta_{(x_1,x_2,\ldots,x_{N-1})}(x_i) = x_{0,i}$ for all $i = 1, \ldots, N-1$.

We can define θ in this way because $\mathbb{R}^2$ is "nice enough". The first point allows us to define an obvious extension

$$\theta : U^{N-1} \times \mathbb{R}^2 \to \mathbb{R}^2$$

by setting $\theta_x(y) = y$ for all $y \notin U$. We also define a homeomorphism

$$\alpha : \mathbb{R}^2 \to \mathbb{R}^2$$

such that

$$\alpha(z_i) = x_{0,i}$$

for all $i = 1, \ldots, N-1$. Again, we can do this because $\mathbb{R}^2$ is "nice enough". We can then find the product structure

$$\pi^{-1}(U^{N-1}) \underset{\phi^{-1}}{\overset{\phi}{\longleftrightarrow}} U^{N-1} \times F_{N-1,1}$$

that we are looking for by setting

$$\begin{aligned}
\phi(x_1, x_2, \ldots, x_{N-1}, y_N) &= (x_1, x_2, \ldots, x_{N-1}, \theta^{-1}_{(x_1,x_2,\ldots,x_{N-1})} \circ \alpha(y_N)) \\
\phi^{-1}(x_1, x_2, \ldots, x_{N-1}, y_N) &= (x_1, x_2, \ldots, x_{N-1}, \alpha^{-1} \circ \theta_{(x_1,x_2,\ldots,x_{N-1})}(y_N))
\end{aligned}$$

Since ϕ is a composition of homeomorphisms, it is a homeomorphism itself. We quickly verify that it is actually well defined on its domain and range. Take a point $(x_1, x_2, \ldots, x_{N-1}, y_N) \in U$. Then we only need to look at

$$\theta^{-1}_{(x_1,x_2,\ldots,x_{N-1})} \circ \alpha(y_N).$$

Now, since y_N can not be any of the gaps z_i, $\alpha(y_N)$ is not any of the $x_{0,i}$, and thus $\theta^{-1} \circ \alpha(y_N)$ is not any of the x_i. Therefore,

$$\phi(x_1, x_2, \ldots, x_{N-1}, y_N) \in \pi^{-1}(U) \subset F_{0,N}.$$

Then for ϕ^{-1}, we look at

$$\alpha^{-1} \circ \theta_{(x_1,x_2,\ldots,x_{N-1})}(y_N)$$

Now y_N may not be equal to any of the x_i, by definition of $F_{0,N}$, so $\theta_{(x_1,x_2,\ldots,x_{N-1})}(y_N)$ is not equal to any of the $x_{0,i}$. Then by our construction, $\alpha^{-1} \circ \theta_{(x_1,x_2,\ldots,x_{N-1})}(y_N)$ is not any of the gaps z_i. And so, our map is well-defined. $\square$

This result is enough for us, but I want to mention the more general result by Fadell and Neuwirth [26]:

Theorem A.3. *The map $\pi : F_{m,N} \to F_{m,R}$ with $N \geq R$, $m \geq 0$, given by*

$$\pi(z_1, \ldots, z_N) = (z_1, \ldots, z_R)$$

is a locally trivial fibration with fibre $F_{m+R,N-R}$.

They suggest the proof for this can be adapted from the proof given for the specific case $R = 1$, which we adapted to find the proof for our specific case: Theorem A.2. With our result, we can use the following lemma, which is a part of Theorem 4.41 in [7], we can formulate a proof for Theorem 2.20. For a proof of this, I refer to the respective theorem in Hatcher.

Lemma A.4. *Let $\tilde{X}, X$ be topological spaces, and let $x_0 \in X$. If $p : \tilde{X} \to X$* has the homotopy lifting property *with resepect to disks D^k for all $k \geq 0$, and if X is path-connected, the sequence*

$$\ldots \longrightarrow \pi_2(\tilde{X}, \tilde{x}_0) \longrightarrow \pi_2(X, x_0) \longrightarrow$$

$$\pi_1(F, \tilde{x}_0) \xrightarrow{i_*} \pi_1(\tilde{X}, \tilde{x}_0) \xrightarrow{p_*} \pi_1(X, x_0) \longrightarrow \pi_0(F, x_0) \longrightarrow \ldots$$

is exact for some homomorphism i_* and the map $p_* : \pi_1(\widetilde{X}, \tilde{x}_0) \to \pi_1(X, x_0)$ induced by p.

Proof. **of Theorem 2.20** Take the map $\pi : F_{0,N} \to F_{0,N-1}$ from Theorem A.2. Using [7, Proposition 4.48] (and since our space is "nice enough"), we can see that we may use Lemma A.4.

I will not go into detail about the n-th order homotopy groups, but essentially instead of considering loops (circles S^1) like we do in π_1, one considers higher dimensional spheres S^n for the group π_n. The group π_0 is related to homotopy of points, and is the group of path components of the given space [6, `Homotopy Group`]. Since the space $F_{N-1,1}$ is clearly path connected, $\pi_0(F_{N-1,1})$ is trivial for any base point.

This solves our issues on the right side of the sequence we are looking for, so we are left to look at the left side. If we think about what it means for the sequence to be exact, we can cut off the left side of the diagram, and replace it by

$$\{\, 1 \,\} \longrightarrow \pi_1(F, \tilde{x}_0)$$

if we can show that the homomorphism $\pi_2(\widetilde{X}, \tilde{x}_0) \to \pi_2(X, x_0)$ is surjective, where $\widetilde{X}$ is $F_{0,N}$ and X is $F_{0,N-1}$. After all, if the homomorphism between these groups is surjective, the kernel of the "next map"

$$\pi_2(X, x_0) \to \pi_1(F, \tilde{x}_0)$$

has to be the entire group $\pi_2(X, x_0)$, and thus the image can only be $\{\, 1 \,\} \subset \pi_1(F, \tilde{x}_0)$, effectively allowing us to simply replace this map by a trivial map from $\{\, 1 \,\}$ to $\pi_1(F, \tilde{x}_0)$.

We show that the map $\pi : F_N \to F_{N-1}$ from Lemma A.4 induces this surjective map, by constructing a *base point preserving* map $g : F_{N-1} \to F_N$ for which $\pi \circ g$ is homotopic to the identity on F_{N-1}. Base point preserving simply means the base point for the fundamental group of the domain F_{N-1} is mapped to the base point of the range F_N.

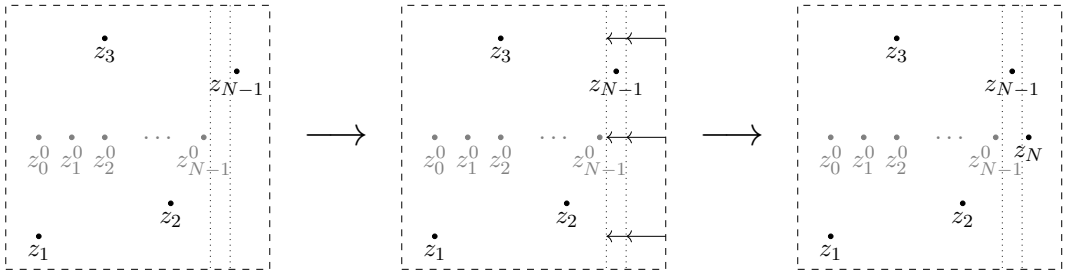

Figure A.1: The base point preserving map $g : F_{N-1} \to F_N$. For a configuration z, the open square that is $\mathbb{R}^2$ is contracted on the right side (denoted by arrows), and the new point in the configuration is placed at z_N^0.

Since $\mathbb{R}^2$ is homeomorphic to the open square $(0,1)^2$, we look at $F_N\left((0,1)^2\right)$ and $F_{N-1}\left((0,1)^2\right)$ instead. First take $z^0 = (z_1^0, \ldots, z_N^0)$ to be the base configuration in $F_N((0,1)^2)$. We call this base configuration for clarity, since z^0 is a tuple of points, but we mean the same. Here, all z_i^0 are evenly spread out on the x-axis. More precisely,

$$z_i^0 = (i/(N+1), 0)$$

for $i = 1, \ldots, N$. Take $\pi(z^0)$ to be the base configuration in $F_{N-1}\left((0,1)^2\right)$. Obviously, π preserves the base point.

The map g is constructed as follows. For any configuration $z \in F_{N-1}\left((0,1)^2\right)$, contract the open square on the right side slightly, and place a new point z_N at z_N^0, where because of the contraction, there are now no points of the configuration. See Figure A.1 for a visual representation of this map. It is clear that this map is well defined, after all, the added point z_N cannot be any of the points $g(z_i)$.

The composition $\pi \circ g$ is homotopic to the identity, since the only thing this map does is a homeomorphic contraction on $\mathbb{R}^2$. It also preserves the base point $\pi(z^0) \in F_{N-1}$. Therefore, the map π is surjective and induces a surjective homomorphism

$$\pi_2(F_N, z^0) \to \pi_2(F_{N-1}, \pi(z^0)),$$

and by our reasoning above, this proves that we may reduce the long exact sequence to

$$\{\,1\,\} \longrightarrow \pi_1(F_{N-1,1}) \xrightarrow{\iota_*} \pi_1(F_N) \xrightarrow{\pi_*} \pi_1(F_{N-1}) \longrightarrow \{\,1\,\}$$

as desired. □

Bibliography

[1] C. Kassel and V. Turaev. *Braid Groups*. Springer-Verlag New York, first edition, 2008.

[2] Frank Wilczek. Quantum mechanics of fractional spin particles. *Phys. Rev. Lett.*, 49:957–959, 1982.

[3] André Joyal and Ross Street. Braided monoidal categories. *MacQuarie Mathematics Reports*, (860081), Nov 1986.

[4] J.M. Leinaas and J. Myrheim. On the theory of identical particles. *Il Nuovo Cimento B*, 37:1–23, 1977. `https://link.springer.com/article/10.1007/BF02727953`.

[5] J.S. Birman. *Braids, Links and Mapping Class Groups (AM-82)*. Princeton University Press, 1975.

[6] nLab. `https://ncatlab.org/nlab/`. Various sub-pages.

[7] A. Hatcher. *Algebraic Topology*. First edition, 2001.

[8] WikiPedia. `https://en.wikipedia.org/`. Various sub-pages.

[9] L. Jacak, P. Sitko, K. Wieczorek, and A. Wòjs. *Quantum Hall Systems*. Oxford University Press, first edition, 2003.

[10] C.H. Jackson. Braid group representations. Master's thesis, Ohio State University, 2001.

[11] G. James and L. Liebeck. *Representations and Gharacters of Groups*. Cambridge University Press, second edition, 2001.

[12] Stephen Bigelow. The burau representation is not faithful for $n = 5$. *Geometry & Topology*, 3(1):397—404, Nov 1999.

[13] Budney R.D. On the image of the Lawrence-Krammer representation. *Journal of Knot Theory and Its Ramifications*, 16:773–789, 2005. `https://arxiv.org/pdf/math/0202246.pdf`.

[14] D. Krammer. Braid groups are linear. *Annals of Mathematics*, 155:131–156, 2002. `https://arxiv.org/pdf/math/0405198.pdf`.

[15] M. Le Bellac. *Quantum Physics*. Cambridge University Press, 2006. Translated by Patricia de Forcrand-Millard.

[16] C. Nash and S. Sen. *Topology and Geometry for Physicists*. Academic Press Inc. (London) LTD., third edition, 1987.

[17] Theodore Frankel. *The Geometry of Physics*. Cambridge University Press, third edition, 2012.

[18] David Tong. Lectures on the quantum hall effect, 2016. `https://arxiv.org/abs/1606.06687`.

[19] D. C. Tsui, H. L. Stormer, and A. C. Gossard. Two-dimensional magnetotransport in the extreme quantum limit. *Phys. Rev. Lett.*, 48:1559–1562, May 1982.

[20] Jainendra K. Jain. *Composite Fermions*. Cambridge University Press, 2007.

[21] David J. Griffiths and Darell F. Schroeter. *Introduction to Quantum Mechanics*. Cambridge University Press, third edition, 2018.

[22] Saunders Mac Lane. *Categories for the Working Mathematician*. Springer-Verlag New York, second edition, 1998.

[23] C. Kassel. *Quantum Groups*. Springer-Verlag New York, first edition, 1995.

[24] F. D. M. Haldane. "Fractional statistics" in arbitrary dimensions: A generalization of the Pauli principle. *Phys. Rev. Lett.*, 67:937–940, Aug 1991.

[25] Dušan Repovš and Pavel Vladimirovič Semenov. *Regular Mappings and Locally Trivial Fibrations*, pages 247–260. Springer Netherlands, Dordrecht, 1998.

[26] E. Fadell and L. Neuwirth. Configuration spaces. *Mathematica Scandinavica*, 10:111–118, 1962. `http://www.mscand.dk/article/download/10517/8538`.